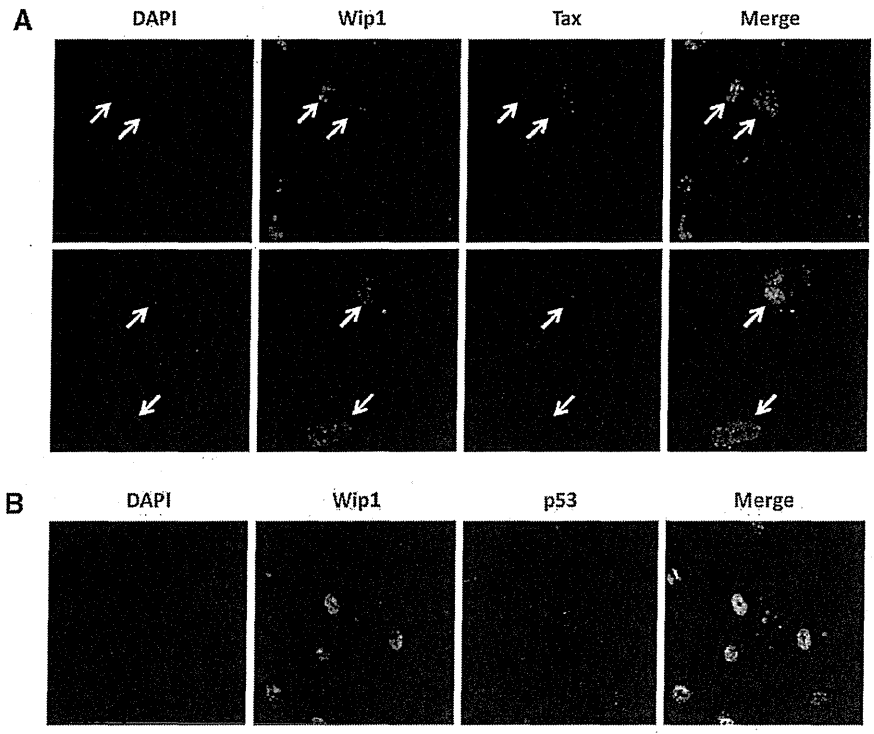

Figure 6 Confocal analyses of p53, Wip1 and Tax in MEF cells. (**A**) Analysis of cell endogenous Wip1 and Tax expression and localization by immunofluorescence staining in MEF cells transfected with a Tax expression plasmid for 48 hours. Cells were stained with anti-Tax (red) and anti-Wip1 (green) antibodies. The nuclei were stained with DAPI (blue). Arrows point to cell that expresses Tax (red) and a neighboring cell that does not express Tax. The same two cells are shown to express equal intensities of Wip1 (green). DAPI (blue) stains cellular nuclei. (**B**) The colocalization of cell endogenous p53 and Wip1 in MEF cells. Cells were stained with anti-p53 (red) or anti-Wip1 (green) antibodies, and DAPI was used to stain nuclei (blue).

viruses; some encode proteins that repress p53 activity. Hence, SV40 large T-antigen stabilizes, but inactivates, p53; adenovirus E1B-55-kDa protein, and the E6 oncoprotein of human papilloma virus (HPV) types 16 and 18 target p53 for ubiquitinylation and degradation [91-93]. In the case of HTLV-1, our work here reaffirms previous findings that Tax indeed attenuates p53's transcriptional activity in cultured cells (Figure 3). However, a perhaps more important implication to arise from our study is that we compare for the first time the impact of Tax inactivation of p53 *versus* p53 inactivation by genetic mutation for their relative contributions to *in vivo* tumorigenesis in mice. To date, it generally has been believed that Tax stringently inactivates p53 activity reducing the need for ATL cells to acquire *p53* inactivating mutations. Our results are, however, incongruent with this notion. Thus, we found that Tax induces tumorigenesis in mice much more robustly in a $p53^{-/-}$ setting than in a $p53^{+/+}$ context (Figure 2A), suggesting that Tax inhibition of p53 in the latter context is significantly less complete than p53 inactivation *via* gene mutation. Our findings differ somewhat from those reported by Portis *et al.* [94]. The differences may be due to variances in the mouse numbers, the mouse strains, and the criteria used to determine tumor-free survival and when euthanasias of mice are performed. To date, in the published literature, only cross-sectional findings are associated between p53 genetic mutations and human ATLLs [54]. These findings do not offer clarity on when p53 mutations occurred relative to HTLV-1 infection, Tax expression, and the onset of transformation of ATLL cells. Our results in mice provide prospective analyses of the contribution of a $p53^{-/-}$ genotype to the initiation of *in vivo* tumorigenesis by Tax. Accordingly, extrapolating our mouse findings to humans suggests that early loss of p53 through a $p53^{-/-}$ genetic mutation in cells infected by HTLV-1 foretells a worse prognosis compared to a corresponding infection in a counterpart $p53^{+/+}$ setting.

In our investigation of p53 inactivation, we report for the first time a contributory role by Wip1 in Tax-tumorigenesis. Our insight into the role of Wip1 arose from the observation that loss of Wip1 (i.e. $Wip1^{-/-}$) significantly reduced the frequency of tumor development in Tax transgenic mice (Figure 4B). We linked this observation to a Wip1-mediated p53 effect because we

found that $Wip1^{-/-}$ MEFs have significantly increased p53 activity over their $Wip1^{+/+}$ counterparts. Thus, a parsimonious interpretation of the collective findings is that loss of Wip1 phosphatase (i.e. $Wip1^{-/-}$) increases cell endogenous p53 activity (Figures 3D and E), and this increase in p53 function reduces Tax-tumorigenicity in $Tax^{+}Wip1^{-/-}$ mice (Figure 4B). Hence, the magnitude of p53 activity is important in regulating the extent of *in vivo* Tax tumorigenesis, and this view is further consistent with the tumor-free survival results comparing $Tax^{+}p53^{+/+}$ and $Tax^{+}p53^{-/-}$ mice (Figure 1).

The potential value of inhibiting Wip1 in moderating cancer progression is not only limited to Tax–induced tumors because a Wip1 effect has also been suggested in mammary gland tumors [95], lymphomas [96], colorectal cancers [97], and other spontaneous tumors [98]. Going forward further clarification is needed to understand whether Wip1's effect on many cancers and its impact on Tax-driven tumor formation are primarily due to its effect on p53 signaling or may also arise from its known effects on other pathways, such as ARF, ATM, and p38 MAPK signaling [96,99]. Studies that compare the *in vivo* tumorigenesis frequencies seen in $Tax^{+}Wip1^{-/-}p53^{-/-}$ versus $Tax^{+}Wip1^{+/+}p53^{-/-}$ mice (two genotypes currently being bred in our laboratory) may help to address whether Wip1 has important substrates other than p53 that contribute to Tax-mediated transformation. In other models of carcinogenesis, it has been shown that the singular over-expression of Wip1 is insufficient to initiate oncogenesis [100] and that Wip1 mostly promotes tumors by cooperating with known oncogenes [100]. Nevertheless, amplification of the *Wip1* gene has been described for numerous human primary tumors [101-112], with virtually all such tumors being genetically p53 wild-type [71,72,113]. Based on this observation, one wonders if the low selective pressure for p53 mutations in ATLL could be due to *Wip1* gene amplification in these cells. To our knowledge, this important question has not yet been investigated in ATLLs.

Conclusions

In summary, despite much progress in HTLV-1 research over the past three decades [114], a salient finding to emerge from this work is the new identification of Wip1 as a cooperating cellular co-factor of Tax in p53-inactivation and *in vivo* tumorigenesis. Currently, our confocal imaging results suggest a colocalization between Tax, Wip1, and p53 within the nucleus (Figure 6 and Additional file 2: Figure S2), but we still lack sufficient data to decipher mechanistically how Tax and Wip1 cooperate to inactivate p53. Amongst several plausible mechanisms, we remain unable to conclude whether Tax can increase Wip1 dephosphorylation of p53 and/or MDM2, a major inhibitor of p53 that has been reported to also be a target of Wip1 [99]. Nonetheless, the functional delineation here of a contribution by Wip1 to Tax tumorigenesis (Figure 4B) does raise the possibility that future uses of small molecule Wip1 phosphatase-inhibitors [115] may benefit ATLL treatment.

Methods

Animals and genotyping

The *Tax* and *Wip1*+/− transgenic mice were previously described [15,74]. The *p53*-mutant mice were purchased from the Jackson lab (strain:B6.129S2-*Trp53tm1Tyj*/J) [68]. The Wip1 and p53 knockout and *Tax* transgenic mice were all generated in C57BL/6 × 129/sv backgrounds [15,68,74]. Genotypes of the mice were determined by polymerase chain reactions (PCRs) using primers: *Tax* (Tax-F-7511-7530: 5′-tcggctcagctctacagttc-3′; Tax-R-8044-8025: 5′-tgagggttgagtggaacgga-3′), *p53* (wt: 5′-acagcgtggtgg taccttat-3′, mutant: 5′-ctatcaggacatagcgttgg-3′ and common: 5′-tatactcagagccggcct-3′) and *Wip1* (Wip1 Exon4 F: 5′-gtggagctatgatttcttcagtgg-3′; Wip1 Exon4 R: 5′-g atacgacacaagacaaacctcc-3′; Wip1 intron 3: 5′-acaagcttg cagggctgtttgtgg-3′; PGK promoter: 5′-cttcccagcctctgagc ccagaaagc-3′). Experimental research on mice follows NIH approved animal study protocols and guidelines.

Analyses of pathologies

Mice were necropsied and examined by mouse pathologists. All of the internal organs (spleen, liver, pancreas, kidney, stomach, intestine, lung, heart, brain, lymph node, thyroid gland) were fixed, paraffin embedded, sectioned and stained with H&E for analyses. Tissues that were found to be grossly abnormal at time of necropsy were multiply sectioned and stained by H&E (hematoxylin and eosin) for microscopic histological analyses.

Cells and reagents

Human cervical cancer cell line HeLa and human colorectal carcinoma cell lines $p53^{+/+}$HCT116 and $p53^{-/-}$HCT116 [81] were cultured in Dulbecco's modified Eagle's medium containing 10% fetal bovine serum (FBS) and antibiotics. Human T cell lines MT2, MT4, C8166, Jurkat, A301, CEM, and H9 were maintained in RPMI 1640 with 10% FBS.

Antibodies

Mouse monoclonal anti-Tax (NIH AIDS Research and Reference Reagent Program) was used to detect Tax protein in immunoblotting and by confocal microscopy. Anti-Flag monoclonal antibody (M2; mouse; Sigma), anti-Wip1 polyclonal antibody (rabbit; Santa Cruz), anti-p53

monoclonal antibody (mouse; Cell Signaling) and anti-tubulin monoclonal antibody (DM1A; mouse; Sigma) were purchased.

Plasmids and transfections

pG13-Luc, p53 (human wild type) (gifts from B. Vogelstein) and Wip1 (gift from L.A. Donehower) expression plasmids were previously described [73,116,117]. HeLa or $p53^{+/+}$ HCT116 or $p53^{-/-}$HCT116 cells were seeded into twelve-well tissue culture plates for the luciferase assays and into 10 cm-dishes for Tax transfections. Transfections were performed 24 h later, using Lipofectamine and Plus reagent (Invitrogen) as described by the manufacturer. At 24 h after transfection of the reporters, cell lysates were subjected to luciferase assay. Total amounts of DNA to be transfected were adjusted by the addition of empty vectors. To detect luciferase and β-Gal activity, luciferase substrate (Promega) and the Galacto-Star assay system (Applied Biosystems) were used. Relative values of luciferase activity were calculated using β-Gal activity as an internal control for transfection.

Real-time PCR

For real-time quantitative reverse transcriptase–polymerase chain reaction (qRTPCR), total cellular RNA from samples was isolated using TriZol reagent according to the manufacturer's instructions (Invitrogen Life technologies). Before reverse transcription, RNA was treated by DNase (Invitrogen) to prevent DNA contamination. First-strand cDNA was synthesized from 1 μg RNA using oligodT and Superscript III reverse transcriptase (Invitrogen). RNA concentration and purity were determined by UV spectrophotometry (nanodrop). The primer pairs were designed using the Universal Probe Library website (Roche diagnostics) (Wip1-L hs: 5′-cccatgttctacaccaccagt-3′; Wip1-R hs: 5′-tggtccttagaatt caccettg-3′; p53-L hs: 5′-ccccagccaaagaagaaac-3′; p53-R hs: 5′-aacatctcgaagcgctcac-3′; p21-L hs: 5′-cgaagtcagttcct tgtggag-3′; p21-R hs: 5′-catgggttctgacggacat-3′). The primers of each pair were located in different exons to avoid genomic amplification. Primer and probe sequences to detect Tax in human T-cells [118] and Tax-SK43: 5′-cggata cccagtctacgtgt-3′ and Tax-SK44: 5′-gagccgataacgcgtccatcg-3′ to detect Tax in mouse spleens. GAPDH was used as the reference gene for he normalization of results (GAPDH-R: 5′-agtgggtgtcgctgttgaag-3′; GAPDH-F: 5′- tgg tatcgtggaaggactca-3′). PCRs were performed using iQSupermix (Bio-Rad) (for quantification of Tax cDNAs in human T-cells) and iQSYBR Green Supermix (for quantification of other cDNAs) on a CFX96 system (Bio-Rad). A large amount of cDNA was prepared from the MT2, C8166, and MT4 cell lines prior to the experiment. This cDNA was 10 fold-diluted, aliquoted and used as a calibrator for Tax and other RT-PCR runs, respectively. For relative quantification and normalization, the comparative Ct (or Eff-DDC) method was used [119].

Immunofluorescence

Cells were cultured on glass coverslips, and fixed in 4% paraformaldehyde at 24 h after transfection. After blocking of nonspecific reactions with 1% bovine serum albumin (BSA), cells were then incubated with the indicated primary antibodies, followed by a subsequent incubation with the secondary antibodies conjugated with Alexa Fluor 488 or 594 (Molecular Probes). DNA was counterstained with 0.1 μg/ml Hoechst 33342. Coverslips were mounted in Prolong Antifade (Molecular Probes), and cells were visualized with a Leica TCS SP2 confocal microscope.

Statistical analyses

The statistical analysis of tumor numbers, survival curves, and spleen weights were computed using the PRISM software (version 5.03).

Additional files

Additional file 1: Figure S1. Analyses of *Tax* mRNA expression in Tax^+ $p53^{-/-}$ and Tax^+ $p53^{+/+}$ mouse spleen tissues. Total RNAs from mouse spleen tissues were extracted and reverse transcribed. The cDNAs were used for real-time RT-PCR analyses of Tax and GAPDH (internal standard) transcripts. The mRNA relative expression levels of Tax mRNA were determined and normalized as multiples of the GAPDH mRNA. There was no statistically significant difference in Tax mRNA expression levels between Tax^+ $p53^{-/-}$ and Tax^+ $p53^{+/+}$ mice (p=0.2758; unpaired *t*-test). Each circle or square represents an independent mouse spleen tissue.

Additional file 2: Figure S2. Confocal analyses of p53, Wip1 and Tax in MEF cells. (A) Analysis of cell endogenous Wip1 and Tax expression and localization by immunofluorescence staining in HCT-116 cells transfected with a Tax expression plasmid for 48 hours. Cells were stained with anti-Tax (red) and anti-Wip1 (green) antibodies. The nuclei were stained with DAPI (blue). Arrows point to cell that expresses Tax (red) and a neighboring cell that does not express Tax. The same two cells are shown to express equal intensities of Wip1 (green). DAPI (blue) stains cellular nuclei. **(B)** The colocalization of cell endogenous p53 and Wip1 in HCT-116 cells. Cells were stained with anti-p53 (red) or anti-Wip1 (green) antibodies, and DAPI was used to stain the nuclei (blue).

Competing interests

The authors declare that they have no competing interests.

Authors' contributions

LZ designed and performed the work, analyzed the data and wrote the paper. YJ started mouse breedings and genotypings. YM performed some genotypings. VY, SWT and CYC contributed reagents and technical advice for the work and edited the paper. LR and XL provided, respectively, Tax and Wip1 mice and participated in discussions. KTJ conceived of the study and supervised the work and wrote the paper. All authors read and approved the final manuscript.

Acknowledgement

This work was supported by intramural NIAID funding. XL was supported by NIH grant R01CA136549. We thank members of the Jeang laboratory for critical readings of the manuscript; Qingpin Liu for her help with mouse tissues and Melissa Foster and Ryan Hamilton for caring of the mice.

Author details
[1]Molecular Virology Section, Laboratory of Molecular Microbiology, the National Institutes of Allergy and Infectious Diseases, the National Institutes of Health, Bethesda, Maryland 20892-0460, USA. [2]Laboratory of Virus Control, Institute for Virus Research, Kyoto University, Kyoto, Japan. [3]Department of Medicine, Washington University School of Medicine, Saint-Louis, Missouri, USA. [4]Department of Cancer Biology, the University of Texas MD Anderson Cancer Center, Houston, Texas, USA.

Received: 16 October 2012 Accepted: 15 December 2012
Published: 21 December 2012

References

1. Proietti FA, Carneiro-Proietti AB, Catalan-Soares BC, Murphy EL: Global epidemiology of HTLV-I infection and associated diseases. *Oncogene* 2005, 24(39):6058–6068.
2. Poiesz BJ, Ruscetti FW, Gazdar AF, Bunn PA, Minna JD, Gallo RC: Detection and isolation of type C retrovirus particles from fresh and cultured lymphocytes of a patient with cutaneous T-cell lymphoma. *Proc Natl Acad Sci U S A* 1980, 77(12):7415–7419.
3. Hinuma Y, Nagata K, Hanaoka M, Nakai M, Matsumoto T, Kinoshita KI, Shirakawa S, Miyoshi I: Adult T-cell leukemia: antigen in an ATL cell line and detection of antibodies to the antigen in human sera. *Proc Natl Acad Sci U S A* 1981, 78(10):6476–6480.
4. Miyoshi I, Kubonishi I, Yoshimoto S, Akagi T, Ohtsuki Y, Shiraishi Y, Nagata K, Hinuma Y: Type C virus particles in a cord T-cell line derived by co-cultivating normal human cord leukocytes and human leukaemic T cells. *Nature* 1981, 294(5843):770–771.
5. Yoshida M, Miyoshi I, Hinuma Y: Isolation and characterization of retrovirus from cell lines of human adult T-cell leukemia and its implication in the disease. *Proc Natl Acad Sci U S A* 1982, 79(6):2031–2035.
6. Watanabe T, Seiki M, Yoshida M: Retrovirus terminology. *Science* 1983, 222(4629):1178.
7. Gallo RC: History of the discoveries of the first human retroviruses: HTLV-1 and HTLV-2. *Oncogene* 2005, 24(39):5926–5930.
8. Goncalves DU, Proietti FA, Barbosa-Stancioli EF, Martins ML, Ribas JG, Martins-Filho OA, Teixeira-Carvalho A, Peruhype-Magalhaes V, Carneiro-Proietti AB: HTLV-1-associated myelopathy/tropical spastic paraparesis (HAM/TSP) inflammatory network. *Inflamm Allergy Drug Targets* 2008, 7(2):98–107.
9. Gessain A, Mahieux R: Tropical spastic paraparesis and HTLV-1 associated myelopathy: clinical, epidemiological, virological and therapeutic aspects. *Rev Neurol (Paris)* 2012, 168(3):257–269.
10. Tanaka A, Takahashi C, Yamaoka S, Nosaka T, Maki M, Hatanaka M: Oncogenic transformation by the tax gene of human T-cell leukemia virus type I in vitro. *Proc Natl Acad Sci U S A* 1990, 87(3):1071–1075.
11. Zane L, Yasunaga J, Kinjo T, de Melo G, Jeang KT: Transformation of human embryonic stem cells by HTLV-1 Tax. *Retrovirology* 2011, 8(Suppl 1):A164.
12. Grassmann R, Berchtold S, Radant I, Alt M, Fleckenstein B, Sodroski JG, Haseltine WA, Ramstedt U: Role of human T-cell leukemia virus type 1 X region proteins in immortalization of primary human lymphocytes in culture. *J Virol* 1992, 66(7):4570–4575.
13. Rosin O, Koch C, Schmitt I, Semmes OJ, Jeang KT, Grassmann R: A human T-cell leukemia virus Tax variant incapable of activating NF-kappaB retains its immortalizing potential for primary T-lymphocytes. *J Biol Chem* 1998, 273(12):6698–6703.
14. Nerenberg M, Hinrichs SH, Reynolds RK, Khoury G, Jay G: The tat gene of human T-lymphotropic virus type 1 induces mesenchymal tumors in transgenic mice. *Science* 1987, 237(4820):1324–1329.
15. Grossman WJ, Kimata JT, Wong FH, Zutter M, Ley TJ, Ratner L: Development of leukemia in mice transgenic for the tax gene of human T-cell leukemia virus type I. *Proc Natl Acad Sci U S A* 1995, 92(4):1057–1061.
16. Hasegawa H, Sawa H, Lewis MJ, Orba Y, Sheehy N, Yamamoto Y, Ichinohe T, Tsunetsugu-Yokota Y, Katano H, Takahashi H, *et al*: Thymus-derived leukemia-lymphoma in mice transgenic for the Tax gene of human T-lymphotropic virus type I. *Nat Med* 2006, 12(4):466–472.
17. Ohsugi T, Kumasaka T, Okada S, Urano T: The Tax protein of HTLV-1 promotes oncogenesis in not only immature T cells but also mature T cells. *Nat Med* 2007, 13(5):527–528.
18. Grassmann R, Aboud M, Jeang KT: Molecular mechanisms of cellular transformation by HTLV-1 Tax. *Oncogene* 2005, 24(39):5976–5985.
19. Matsuoka M, Jeang KT: Human T-cell leukemia virus type 1 (HTLV-1) and leukemic transformation: viral infectivity, Tax, HBZ and therapy. *Oncogene* 2011, 30(12):1379–1389.
20. Zane L, Sibon D, Jeannin L, Zandecki M, Delfau-Larue MH, Gessain A, Gout O, Pinatel C, Lancon A, Mortreux F, *et al*: Tax gene expression and cell cycling but not cell death are selected during HTLV-1 infection in vivo. *Retrovirology* 2010, 7:17.
21. Jeang KT, Boros I, Brady J, Radonovich M, Khoury G: Characterization of cellular factors that interact with the human T-cell leukemia virus type I p40x-responsive 21-base-pair sequence. *J Virol* 1988, 62(12):4499–4509.
22. Goren I, Semmes OJ, Jeang KT, Moelling K: The amino terminus of Tax is required for interaction with the cyclic AMP response element binding protein. *J Virol* 1995, 69(9):5806–5811.
23. Tie F, Adya N, Greene WC, Giam CZ: Interaction of the human T-lymphotropic virus type 1 Tax dimer with CREB and the viral 21-base-pair repeat. *J Virol* 1996, 70(12):8368–8374.
24. Harrod R, Tang Y, Nicot C, Lu HS, Vassilev A, Nakatani Y, Giam CZ: An exposed KID-like domain in human T-cell lymphotropic virus type 1 Tax is responsible for the recruitment of coactivators CBP/p300. *Mol Cell Biol* 1998, 18(9):5052–5061.
25. Harhaj EW, Sun SC: IKKgamma serves as a docking subunit of the IkappaB kinase (IKK) and mediates interaction of IKK with the human T-cell leukemia virus Tax protein. *J Biol Chem* 1999, 274(33):22911–22914.
26. Xiao G, Cvijic ME, Fong A, Harhaj EW, Uhlik MT, Waterfield M, Sun SC: Retroviral oncoprotein Tax induces processing of NF-kappaB2/p100 in T cells: evidence for the involvement of IKKalpha. *EMBO J* 2001, 20(23):6805–6815.
27. Iha H, Kibler KV, Yedavalli VR, Peloponese JM, Haller K, Miyazato A, Kasai T, Jeang KT: Segregation of NF-kappaB activation through NEMO/IKKgamma by Tax and TNFalpha: implications for stimulus-specific interruption of oncogenic signaling. *Oncogene* 2003, 22(55):8912–8923.
28. Qu Z, Xiao G: Human T-cell lymphotropic virus: a model of NF-kappaB-associated tumorigenesis. *Viruses* 2011, 3(6):714–749.
29. Fu DX, Kuo YL, Liu BY, Jeang KT, Giam CZ: Human T-lymphotropic virus type I tax activates I-kappa B kinase by inhibiting I-kappa B kinase-associated serine/threonine protein phosphatase 2A. *J Biol Chem* 2003, 278(3):1487–1493.
30. Iwanaga R, Ohtani K, Hayashi T, Nakamura M: Molecular mechanism of cell cycle progression induced by the oncogene product Tax of human T-cell leukemia virus type I. *Oncogene* 2001, 20(17):2055–2067.
31. Haller K, Wu Y, Derow E, Schmitt I, Jeang KT, Grassmann R: Physical interaction of human T-cell leukemia virus type 1 Tax with cyclin-dependent kinase 4 stimulates the phosphorylation of retinoblastoma protein. *Mol Cell Biol* 2002, 22(10):3327–3338.
32. Fraedrich K, Muller B, Grassmann R: The HTLV-1 Tax protein binding domain of cyclin-dependent kinase 4 (CDK4) includes the regulatory PSTAIRE helix. *Retrovirology* 2005, 2:54.
33. Neuveut C, Low KG, Maldarelli F, Schmitt I, Majone F, Grassmann R, Jeang KT: Human T-cell leukemia virus type 1 Tax and cell cycle progression: role of cyclin D-cdk and p110Rb. *Mol Cell Biol* 1998, 18(6):3620–3632.
34. Jeong SJ, Dasgupta A, Jung KJ, Um JH, Burke A, Park HU, Brady JN: PI3K/AKT inhibition induces caspase-dependent apoptosis in HTLV-1-transformed cells. *Virology* 2008, 370(2):264–272.
35. Liu Y, Wang Y, Yamakuchi M, Masuda S, Tokioka T, Yamaoka S, Maruyama I, Kitajima I: Phosphoinositide-3 kinase-PKB/Akt pathway activation is involved in fibroblast Rat-1 transformation by human T-cell leukemia virus type I tax. *Oncogene* 2001, 20(20):2514–2526.
36. Peloponese JM Jr, Jeang KT: Role for Akt/protein kinase B and activator protein-1 in cellular proliferation induced by the human T-cell leukemia virus type 1 tax oncoprotein. *J Biol Chem* 2006, 281(13):8927–8938.
37. Majone F, Semmes OJ, Jeang KT: Induction of micronuclei by HTLV-I Tax: a cellular assay for function. *Virology* 1993, 193(1):456–459.
38. Semmes OJ, Majone F, Cantemir C, Turchetto L, Hjelle B, Jeang KT: HTLV-I and HTLV-II Tax: differences in induction of micronuclei in cells and transcriptional activation of viral LTRs. *Virology* 1996, 217(1):373–379.
39. Kinjo T, Ham-Terhune J, Peloponese JM Jr, Jeang KT: Induction of reactive oxygen species by human T-cell leukemia virus type 1 tax correlates with DNA damage and expression of cellular senescence marker. *J Virol* 2010, 84(10):5431–5437.

40. Majone F, Jeang KT: Unstabilized DNA breaks in HTLV-1 Tax expressing cells correlate with functional targeting of Ku80, not PKcs, XRCC4, or H2AX. *Cell Biosci* 2012, 2(1):15.
41. Durkin SS, Guo X, Fryrear KA, Mihaylova VT, Gupta SK, Belgnaoui SM, Haoudi A, Kupfer GM, Semmes OJ: HTLV-1 Tax oncoprotein subverts the cellular DNA damage response via binding to DNA-dependent protein kinase. *J Biol Chem* 2008, 283(52):36311–36320.
42. Gatza ML, Dayaram T, Marriott SJ: Ubiquitination of HTLV-I Tax in response to DNA damage regulates nuclear complex formation and nuclear export. *Retrovirology* 2007, 4:95.
43. Hanahan D, Weinberg RA: The hallmarks of cancer. *Cell* 2000, 100(1):57–70.
44. Hanahan D, Weinberg RA: Hallmarks of cancer: the next generation. *Cell* 2011, 144(5):646–674.
45. Jin DY, Spencer F, Jeang KT: Human T cell leukemia virus type 1 oncoprotein Tax targets the human mitotic checkpoint protein MAD1. *Cell* 1998, 93(1):81–91.
46. Yasunaga J, Jeang KT: Viral transformation and aneuploidy. *Environ Mol Mutagen* 2009, 50(8):733–740.
47. Vousden KH, Lu X: Live or let die: the cell's response to p53. *Nat Rev Cancer* 2002, 2(8):594–604.
48. Zenz T, Benner A, Dohner H, Stilgenbauer S: Chronic lymphocytic leukemia and treatment resistance in cancer: the role of the p53 pathway. *Cell Cycle* 2008, 7(24):3810–3814.
49. Freed-Pastor WA, Prives C: Mutant p53: one name, many proteins. *Genes Dev* 2012, 26(12):1268–1286.
50. Xu-Monette ZY, Medeiros LJ, Li Y, Orlowski RZ, Andreeff M, Bueso-Ramos CE, Greiner TC, McDonnell TJ, Young KH: Dysfunction of the TP53 tumor suppressor gene in lymphoid malignancies. *Blood* 2012, 119(16):3668–3683.
51. Toyooka S, Tsuda T, Gazdar AF: The TP53 gene, tobacco exposure, and lung cancer. *Hum Mutat* 2003, 21(3):229–239.
52. Iacopetta B: TP53 mutation in colorectal cancer. *Hum Mutat* 2003, 21(3):271–276.
53. Hatta Y, Koeffler HP: Role of tumor suppressor genes in the development of adult T cell leukemia/lymphoma (ATLL). *Leukemia* 2002, 16(6):1069–1085.
54. Tawara M, Hogerzeil SJ, Yamada Y, Takasaki Y, Soda H, Hasegawa H, Murata K, Ikeda S, Imaizumi Y, Sugahara K, *et al*: Impact of p53 aberration on the progression of Adult T-cell Leukemia/Lymphoma. *Cancer Lett* 2006, 234(2):249–255.
55. Tabakin-Fix Y, Azran I, Schavinky-Khrapunsky Y, Levy O, Aboud M: Functional inactivation of p53 by human T-cell leukemia virus type 1 Tax protein: mechanisms and clinical implications. *Carcinogenesis* 2006, 27(4):673–681.
56. Nagai H, Kinoshita T, Imamura J, Murakami Y, Hayashi K, Mukai K, Ikeda S, Tobinai K, Saito H, Shimoyama M, *et al*: Genetic alteration of p53 in some patients with adult T-cell leukemia. *Jpn J Cancer Res* 1991, 82(12):1421–1427.
57. Sakashita A, Hattori T, Miller CW, Suzushima H, Asou N, Takatsuki K, Koeffler HP: Mutations of the p53 gene in adult T-cell leukemia. *Blood* 1992, 79(2):477–480.
58. Reid RL, Lindholm PF, Mireskandari A, Dittmer J, Brady JN: Stabilization of wild-type p53 in human T-lymphocytes transformed by HTLV-I. *Oncogene* 1993, 8(11):3029–3036.
59. Pise-Masison CA, Choi KS, Radonovich M, Dittmer J, Kim SJ, Brady JN: Inhibition of p53 transactivation function by the human T-cell lymphotropic virus type 1 Tax protein. *J Virol* 1998, 72(2):1165–1170.
60. Pise-Masison CA, Radonovich M, Sakaguchi K, Appella E, Brady JN: Phosphorylation of p53: a novel pathway for p53 inactivation in human T-cell lymphotropic virus type 1-transformed cells. *J Virol* 1998, 72(8):6348–6355.
61. Akagi T, Ono H, Tsuchida N, Shimotohno K: Aberrant expression and function of p53 in T-cells immortalized by HTLV-I Tax1. *FEBS Lett* 1997, 406(3):263–266.
62. Ariumi Y, Kaida A, Lin JY, Hirota M, Masui O, Yamaoka S, Taya Y, Shimotohno K: HTLV-1 tax oncoprotein represses the p53-mediated trans-activation function through coactivator CBP sequestration. *Oncogene* 2000, 19(12):1491–1499.
63. Pise-Masison CA, Mahieux R, Radonovich M, Jiang H, Brady JN: Human T-lymphotropic virus type I Tax protein utilizes distinct pathways for p53 inhibition that are cell type-dependent. *J Biol Chem* 2001, 276(1):200–205.
64. Van PL, Yim KW, Jin DY, Dapolito G, Kurimasa A, Jeang KT: Genetic evidence of a role for ATM in functional interaction between human T-cell leukemia virus type 1 Tax and p53. *J Virol* 2001, 75(1):396–407.
65. Miyazato A, Sheleg S, Iha H, Li Y, Jeang KT: Evidence for NF-kappaB- and CBP-independent repression of p53's transcriptional activity by human T-cell leukemia virus type 1 Tax in mouse embryo and primary human fibroblasts. *J Virol* 2005, 79(14):9346–9350.
66. Pise-Masison CA, Mahieux R, Jiang H, Ashcroft M, Radonovich M, Duvall J, Guillerm C, Brady JN: Inactivation of p53 by human T-cell lymphotropic virus type 1 Tax requires activation of the NF-kappaB pathway and is dependent on p53 phosphorylation. *Mol Cell Biol* 2000, 20(10):3377–3386.
67. Jeong SJ, Radonovich M, Brady JN, Pise-Masison CA: HTLV-I Tax induces a novel interaction between p65/RelA and p53 that results in inhibition of p53 transcriptional activity. *Blood* 2004, 104(5):1490–1497.
68. Jacks T, Remington L, Williams BO, Schmitt EM, Halachmi S, Bronson RT, Weinberg RA: Tumor spectrum analysis in p53-mutant mice. *Curr Biol* 1994, 4(1):1–7.
69. Chi YH, Ward JM, Cheng LI, Yasunaga J, Jeang KT: Spindle assembly checkpoint and p53 deficiencies cooperate for tumorigenesis in mice. *Int J Cancer* 2009, 124(6):1483–1489.
70. Fiscella M, Zhang H, Fan S, Sakaguchi K, Shen S, Mercer WE, Vande Woude GF, O'Connor PM, Appella E: Wip1, a novel human protein phosphatase that is induced in response to ionizing radiation in a p53-dependent manner. *Proc Natl Acad Sci U S A* 1997, 94(12):6048–6053.
71. Bulavin DV, Demidov ON, Saito S, Kauraniemi P, Phillips C, Amundson SA, Ambrosino C, Sauter G, Nebreda AR, Anderson CW, *et al*: Amplification of PPM1D in human tumors abrogates p53 tumor-suppressor activity. *Nat Genet* 2002, 31(2):210–215.
72. Yu E, Ahn YS, Jang SJ, Kim MJ, Yoon HS, Gong G, Choi J: Overexpression of the wip1 gene abrogates the p38 MAPK/p53/Wip1 pathway and silences p16 expression in human breast cancers. *Breast Cancer Res Treat* 2007, 101(3):269–278.
73. el-Deiry WS, Kern SE, Pietenpol JA, Kinzler KW, Vogelstein B: Definition of a consensus binding site for p53. *Nat Genet* 1992, 1(1):45–49.
74. Choi J, Nannenga B, Demidov ON, Bulavin DV, Cooney A, Brayton C, Zhang Y, Mbawuike IN, Bradley A, Appella E, *et al*: Mice deficient for the wild-type p53-induced phosphatase gene (Wip1) exhibit defects in reproductive organs, immune function, and cell cycle control. *Mol Cell Biol* 2002, 22(4):1094–1105.
75. Waldele K, Silbermann K, Schneider G, Ruckes T, Cullen BR, Grassmann R: Requirement of the human T-cell leukemia virus (HTLV-1) tax-stimulated HIAP-1 gene for the survival of transformed lymphocytes. *Blood* 2006, 107(11):4491–4499.
76. Pichler K, Kattan T, Gentzsch J, Kress AK, Taylor GP, Bangham CR, Grassmann R: Strong induction of 4-1BB, a growth and survival promoting costimulatory receptor, in HTLV-1-infected cultured and patients' T cells by the viral Tax oncoprotein. *Blood* 2008, 111(9):4741–4751.
77. Krueger A, Fas SC, Giaisi M, Bleumink M, Merling A, Stumpf C, Baumann S, Holtkotte D, Bosch V, Krammer PH, *et al*: HTLV-1 Tax protects against CD95-mediated apoptosis by induction of the cellular FLICE-inhibitory protein (c-FLIP). *Blood* 2006, 107(10):3933–3939.
78. Jeang KT, Widen SG, Semmes OJ, Wilson SH: HTLV-I trans-activator protein, tax, is a trans-repressor of the human beta-polymerase gene. *Science* 1990, 247(4946):1082–1084.
79. Zhang J, Yamada O, Kida S, Matsushita Y, Yamaoka S, Chagan-Yasutan H, Hattori T: Identification of CD44 as a downstream target of noncanonical NF-kappaB pathway activated by human T-cell leukemia virus type 1-encoded Tax protein. *Virology* 2011, 413(2):244–252.
80. Zane L, Sibon D, Legras C, Lachuer J, Wierinckx A, Mehlen P, Delfau-Larue MH, Gessain A, Gout O, Pinatel C, *et al*: Clonal expansion of HTLV-1 positive CD8+ cells relies on cIAP-2 but not on c-FLIP expression. *Virology* 2010, 407(2):341–351.
81. Bunz F, Dutriaux A, Lengauer C, Waldman T, Zhou S, Brown JP, Sedivy JM, Kinzler KW, Vogelstein B: Requirement for p53 and p21 to sustain G2 arrest after DNA damage. *Science* 1998, 282(5393):1497–1501.
82. Vogelstein B, Lane D, Levine AJ: Surfing the p53 network. *Nature* 2000, 408(6810):307–310.
83. Petitjean A, Achatz MI, Borresen-Dale AL, Hainaut P, Olivier M: TP53 mutations in human cancers: functional selection and impact on cancer prognosis and outcomes. *Oncogene* 2007, 26(15):2157–2165.

84. Petitjean A, Mathe E, Kato S, Ishioka C, Tavtigian SV, Hainaut P, Olivier M: Impact of mutant p53 functional properties on TP53 mutation patterns and tumor phenotype: lessons from recent developments in the IARC TP53 database. *Hum Mutat* 2007, 28(6):622–629.
85. Levine AJ, Oren M: The first 30 years of p53: growing ever more complex. *Nat Rev Cancer* 2009, 9(10):749–758.
86. Polager S, Ginsberg D: p53 and E2f: partners in life and death. *Nat Rev Cancer* 2009, 9(10):738–748.
87. Poyurovsky MV, Prives C: Unleashing the power of p53: lessons from mice and men. *Genes Dev* 2006, 20(2):125–131.
88. Manfredi JJ: The Mdm2-p53 relationship evolves: Mdm2 swings both ways as an oncogene and a tumor suppressor. *Genes Dev* 2010, 24(15):1580–1589.
89. Marine JC, Lozano G: Mdm2-mediated ubiquitylation: p53 and beyond. *Cell Death Differ* 2010, 17(1):93–102.
90. Piccinin S, Tonin E, Sessa S, Demontis S, Rossi S, Pecciarini L, Zanatta L, Pivetta F, Grizzo A, Sonego M, *et al*: A "Twist box" Code of p53 Inactivation: Twist box:p53 Interaction Promotes p53 Degradation. *Cancer Cell* 2012, 22(3):404–415.
91. Levine AJ: The common mechanisms of transformation by the small DNA tumor viruses: the inactivation of tumor suppressor gene products: p53. *Virology* 2009, 384(2):285–293.
92. Atkin SJ, Griffin BE, Dilworth SM: Polyoma virus and simian virus 40 as cancer models: history and perspectives. *Semin Cancer Biol* 2009, 19(4):211–217.
93. Gao P, Zheng J: Oncogenic virus-mediated cell fusion: new insights into initiation and progression of oncogenic viruses–related cancers. *Cancer Lett* 2011, 303(1):1–8.
94. Portis T, Grossman WJ, Harding JC, Hess JL, Ratner L: Analysis of p53 inactivation in a human T-cell leukemia virus type 1 Tax transgenic mouse model. *J Virol* 2001, 75(5):2185–2193.
95. Bulavin DV, Phillips C, Nannenga B, Timofeev O, Donehower LA, Anderson CW, Appella E, Fornace AJ Jr: Inactivation of the Wip1 phosphatase inhibits mammary tumorigenesis through p38 MAPK-mediated activation of the p16(Ink4a)-p19(Arf) pathway. *Nat Genet* 2004, 36(4):343–350.
96. Shreeram S, Hee WK, Demidov ON, Kek C, Yamaguchi H, Fornace AJ Jr, Anderson CW, Appella E, Bulavin DV: Regulation of ATM/p53-dependent suppression of myc-induced lymphomas by Wip1 phosphatase. *J Exp Med* 2006, 203(13):2793–2799.
97. Demidov ON, Timofeev O, Lwin HN, Kek C, Appella E, Bulavin DV: Wip1 phosphatase regulates p53-dependent apoptosis of stem cells and tumorigenesis in the mouse intestine. *Cell Stem Cell* 2007, 1(2):180–190.
98. Nannenga B, Lu X, Dumble M, Van Maanen M, Nguyen TA, Sutton R, Kumar TR, Donehower LA: Augmented cancer resistance and DNA damage response phenotypes in PPM1D null mice. *Mol Carcinog* 2006, 45(8):594–604.
99. Lu X, Nguyen TA, Moon SH, Darlington Y, Sommer M, Donehower LA: The type 2C phosphatase Wip1: an oncogenic regulator of tumor suppressor and DNA damage response pathways. *Cancer Metastasis Rev* 2008, 27(2):123–135.
100. Demidov ON, Kek C, Shreeram S, Timofeev O, Fornace AJ, Appella E, Bulavin DV: The role of the MKK6/p38 MAPK pathway in Wip1-dependent regulation of ErbB2-driven mammary gland tumorigenesis. *Oncogene* 2007, 26(17):2502–2506.
101. Li J, Yang Y, Peng Y, Austin RJ, van Eyndhoven WG, Nguyen KC, Gabriele T, McCurrach ME, Marks JR, Hoey T, *et al*: Oncogenic properties of PPM1D located within a breast cancer amplification epicenter at 17q23. *Nat Genet* 2002, 31(2):133–134.
102. Sinclair CS, Rowley M, Naderi A, Couch FJ: The 17q23 amplicon and breast cancer. *Breast Cancer Res Treat* 2003, 78(3):313–322.
103. Barlund M, Kuukasjarvi T, Syrjakoski K, Auvinen A, Kallioniemi A: Frequent amplification and overexpression of CCND1 in male breast cancer. *Int J Cancer* 2004, 111(6):968–971.
104. Tan DS, Lambros MB, Rayter S, Natrajan R, Vatcheva R, Gao Q, Marchio C, Geyer FC, Savage K, Parry S, *et al*: PPM1D is a potential therapeutic target in ovarian clear cell carcinomas. *Clin Cancer Res* 2009, 15(7):2269–2280.
105. Natrajan R, Lambros MB, Rodriguez-Pinilla SM, Moreno-Bueno G, Tan DS, Marchio C, Vatcheva R, Rayter S, Mahler-Araujo B, Fulford LG, *et al*: Tiling path genomic profiling of grade 3 invasive ductal breast cancers. *Clin Cancer Res* 2009, 15(8):2711–2722.
106. Saito-Ohara F, Imoto I, Inoue J, Hosoi H, Nakagawara A, Sugimoto T, Inazawa J: PPM1D is a potential target for 17q gain in neuroblastoma. *Cancer Res* 2003, 63(8):1876–1883.
107. Castellino RC, De Bortoli M, Lu X, Moon SH, Nguyen TA, Shepard MA, Rao PH, Donehower LA, Kim JY: Medulloblastomas overexpress the p53-inactivating oncogene WIP1/PPM1D. *J Neurooncol* 2008, 86(3):245–256.
108. Mendrzyk F, Radlwimmer B, Joos S, Kokocinski F, Benner A, Stange DE, Neben K, Fiegler H, Carter NP, Reifenberger G, *et al*: Genomic and protein expression profiling identifies CDK6 as novel independent prognostic marker in medulloblastoma. *J Clin Oncol* 2005, 23(34):8853–8862.
109. Ehrbrecht A, Muller U, Wolter M, Hoischen A, Koch A, Radlwimmer B, Actor B, Mincheva A, Pietsch T, Lichter P, *et al*: Comprehensive genomic analysis of desmoplastic medulloblastomas: identification of novel amplified genes and separate evaluation of the different histological components. *J Pathol* 2006, 208(4):554–563.
110. Hirasawa A, Saito-Ohara F, Inoue J, Aoki D, Susumu N, Yokoyama T, Nozawa S, Inazawa J, Imoto I: Association of 17q21-q24 gain in ovarian clear cell adenocarcinomas with poor prognosis and identification of PPM1D and APPBP2 as likely amplification targets. *Clin Cancer Res* 2003, 9(6):1995–2004.
111. Fuku T, Semba S, Yutori H, Yokozaki H: Increased wild-type p53-induced phosphatase 1 (Wip1 or PPM1D) expression correlated with downregulation of checkpoint kinase 2 in human gastric carcinoma. *Pathol Int* 2007, 57(9):566–571.
112. Loukopoulos P, Shibata T, Katoh H, Kokubu A, Sakamoto M, Yamazaki K, Kosuge T, Kanai Y, Hosoda F, Imoto I, *et al*: Genome-wide array-based comparative genomic hybridization analysis of pancreatic adenocarcinoma: identification of genetic indicators that predict patient outcome. *Cancer Sci* 2007, 98(3):392–400.
113. Rauta J, Alarmo EL, Kauraniemi P, Karhu R, Kuukasjarvi T, Kallioniemi A: The serine-threonine protein phosphatase PPM1D is frequently activated through amplification in aggressive primary breast tumours. *Breast Cancer Res Treat* 2006, 95(3):257–263.
114. Martin F, Bangham CR, Ciminale V, Lairmore MD, Murphy EL, Switzer WM, Mahieux R: Conference highlights of the 15th International Conference on Human Retrovirology: HTLV and related retroviruses, 4–8 June 2011, Leuven, Gembloux, Belgium. *Retrovirology* 2011, 8:86.
115. Hayashi R, Tanoue K, Durell SR, Chatterjee DK, Jenkins LM, Appella DH, Appella E: Optimization of a cyclic peptide inhibitor of Ser/Thr phosphatase PPM1D (Wip1). *Biochemistry* 2011, 50(21):4537–4549.
116. Kern SE, Pietenpol JA, Thiagalingam S, Seymour A, Kinzler KW, Vogelstein B: Oncogenic forms of p53 inhibit p53-regulated gene expression. *Science* 1992, 256(5058):827–830.
117. Choi J, Appella E, Donehower LA: The structure and expression of the murine wildtype p53-induced phosphatase 1 (Wip1) gene. *Genomics* 2000, 64(3):298–306.
118. Yamano Y, Nagai M, Brennan M, Mora CA, Soldan SS, Tomaru U, Takenouchi N, Izumo S, Osame M, Jacobson S: Correlation of human T-cell lymphotropic virus type 1 (HTLV-1) mRNA with proviral DNA load, virus-specific CD8(+) T cells, and disease severity in HTLV-1-associated myelopathy (HAM/TSP). *Blood* 2002, 99(1):88–94.
119. Livak KJ, Schmittgen TD: Analysis of relative gene expression data using real-time quantitative PCR and the 2(–Delta Delta C(T)) Method. *Methods* 2001, 25(4):402–408.

doi:10.1186/1742-4690-9-114
Cite this article as: Zane *et al.*: Wip1 and p53 contribute to HTLV-1 Tax-induced tumorigenesis. *Retrovirology* 2012 9:114.

Oncogene (2013) 32, 4222–4230

www.nature.com/onc

ORIGINAL ARTICLE

HTLV-1 bZIP factor dysregulates the Wnt pathways to support proliferation and migration of adult T-cell leukemia cells

G Ma[1], J Yasunaga[1], J Fan[1], S Yanagawa[2] and M Matsuoka[1]

Human T-cell leukemia virus type 1 (HTLV-1) is the causative agent of adult T-cell leukemia (ATL). HTLV-1 bZIP factor (HBZ), the viral gene transcribed from the antisense strand, is consistently expressed in ATL cells and promotes their proliferation. In this study, we found that a Wnt pathway-related protein, disheveled-associating protein with a high frequency of leucine residues (DAPLE), interacts with both HTLV-1 Tax and HBZ. In the presence of DAPLE, Tax activated canonical Wnt signaling. Conversely, HBZ markedly suppressed canonical Wnt activation induced by either Tax/DAPLE or β-catenin. As a mechanism of HBZ-mediated Wnt suppression, we found that HBZ targets lymphoid enhancer-binding factor 1, one of the key transcription factors of the pathway, and impairs its DNA-binding ability. We also observed that the canonical Wnt pathway was not activated in HTLV-1-infected cells, whereas the representative of noncanonical Wnt ligand, Wnt5a, which antagonizes canonical Wnt signaling, was overexpressed. HBZ was able to induce Wnt5a transcription by enhancing its promoter activity through the TGF-β pathway. Importantly, knocking down of Wnt5a in ATL cells repressed cellular proliferation and migration. Our results implicate novel roles of HBZ in ATL leukemogenesis through dysregulation of both the canonical and noncanonical Wnt pathways.

Oncogene (2013) **32,** 4222–4230; doi:10.1038/onc.2012.450; published online 8 October 2012

Keywords: HTLV-1; HBZ; Tax; DAPLE; Wnt signaling pathway; Wnt5a

INTRODUCTION

Human T-cell leukemia virus type 1 (HTLV-1) is the causative agent of adult T-cell leukemia (ATL).[1–5] HTLV-1 Tax is an important viral transactivator, and has been thought to have a key role in the pathogenesis of HTLV-1.[5,6] However, the finding that expression of functional Tax cannot be detected in ~60% of fresh ATL cases indicates that other viral and/or cellular factors might also be implicated.[5,7] We have reported that HTLV-1 bZIP factor (HBZ), which is encoded by the minus strand of the HTLV-1 provirus, promotes proliferation of ATL cells and is consistently expressed in all ATL cells.[8,9] Recently, we also demonstrated that HBZ transgenic mice developed T-cell lymphomas and systemic inflammation,[10] indicating that HBZ has an oncogenic property and has important roles in HTLV-1-associated pathogenesis.

The Wnt signaling is a highly conserved cellular signaling pathway in eukaryotes and has critical roles in embryonic development and tissue homeostasis.[11] To date, 19 Wnt ligands have been discovered and found to trigger the multiple pathways of Wnt signaling.[11] The most well-studied cascade is the so-called canonical Wnt pathway (also known as the Wnt/β-catenin pathway), which is β-catenin-dependent and mainly controls cell differentiation, proliferation and apoptosis.[12] In the absence of the canonical Wnt ligands, cytosolic β-catenin is subjected to a destruction complex consisting of axis inhibitor, adenomatous polyposis coli, glycogen-synthase kinase 3β and casein kinase 1, phosphorylated at Ser45/Thr41/Ser37/33 by casein kinase 1/glycogen-synthase kinase 3β and finally degraded by a proteasome.[12] When a canonical Wnt ligand exists, it binds to low-density lipoprotein-receptor-related protein and frizzled membrane coreceptors and triggers the recruitment of disheveled (Dvl) to the membrane, which then binds to axis inhibitor, and thus prevents the formation of the destruction complex. Consequently, free cytosolic β-catenin accumulates and is translocated into the nucleus, where it binds to T-cell factor/lymphoid enhancer-binding factor (TCF/LEF) and coactivates the transcription of target genes.[12,13] Other branches of Wnt signaling, such as the Wnt-Ca^{2+} or planar cell polarity pathway, are generally referred to as the noncanonical Wnt pathway, which might only need frizzled membrane as a single receptor and does not signal through β-catenin.[13] It is well accepted that the noncanonical Wnt ligands antagonize the canonical Wnt pathway, although the mechanism is not clearly defined.[14]

So far, aberrant activation of the canonical Wnt pathway has been linked to many cancers, including some virus-induced malignancies, such as hepatocellular carcinoma, Kaposi's sarcoma and cervical cancer.[15–19] It is also involved in hematological malignancies.[20–23] However, its roles in ATL have not been clarified. In this study, we demonstrate that the canonical Wnt pathway is actually not activated in HTLV-1-infected cells; in addition, HBZ suppresses it through interacting with LEF1 and impairing its DNA-binding ability. Meanwhile, HBZ upregulates the expression of the noncanonical Wnt5a by enhancing its promoter activity. Knockdown of Wnt5a impairs both proliferation and migration of ATL cells, indicating that perturbation of the Wnt signaling pathways by HBZ is associated with the leukemogenesis of ATL.

RESULTS

HBZ counteracts the canonical Wnt activation induced by Tax

Previously, we identified several cellular candidates of the HBZ interactants by yeast two-hybrid screening.[24] Among them,

[1]Laboratory of Virus Control, Institute for Virus Research, Kyoto University, Kyoto, Japan and [2]Laboratory of Gene Analysis, Institute for Virus Research, Kyoto University, Kyoto, Japan. Correspondence: Dr J Yasunaga, Laboratory of Virus Control, Institute for Virus Research, Kyoto University, 53 Shogoin Kawahara-cho, Kyoto 606-8507, Japan.
E-mail: jyasunag@virus.kyoto-u.ac.jp
Received 8 June 2012; revised 2 August 2012; accepted 10 August 2012; published online 8 October 2012

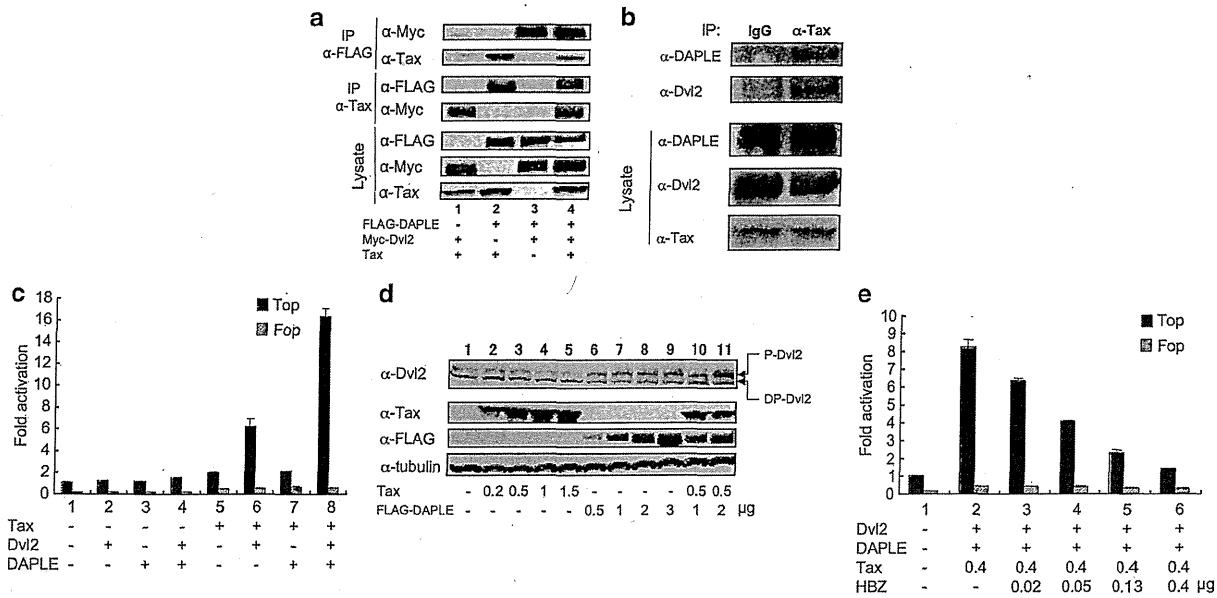

Figure 1. HBZ counteracts the canonical Wnt activation induced by Tax. (**a**) Co-IP analysis of the interaction among DAPLE, Tax and Dvl2 in 293FT cells. (**b**) Co-IP analysis of the association of endogenous Tax and DAPLE/Dvl2 in ATL-T cells. (**c**) Effects of Tax, Dvl2 and DAPLE on the canonical Wnt pathway. (**d**) Effects of overexpression of Tax and DAPLE on the endogenous Dvl2 expression in 293FT cells. P-Dvl2 indicates phosphorylated form and DP-Dvl2 indicates dephosphorylated form of Dvl2, respectively. (**e**) Effects of HBZ on Tax/Dvl2/DAPLE-induced canonical Wnt activation.

we focused on one protein named Dvl-associating protein with a high frequency of leucine residues (DAPLE) for two reasons; first, it is a bZIP protein, suggesting that it can hetero-dimerize with HBZ through their bZIP domains. Second, it has been reported that this protein is associated with the Wnt/β-catenin pathway,[25] which is a well-studied oncogenic signaling pathway. In our initial experiment, we overexpressed HBZ and DAPLE in 293FT cells and confirmed their interaction by co-immunoprecipitation (Co-IP) assay (Supplementary Figure S1). In some previous studies, it has been shown that HTLV-1 Tax and HBZ target the same cellular molecules, such as NF-κB p65, CREB and p300/CBP, but exhibit opposite effects.[26–29] So we next asked if Tax also interacts with DAPLE and has any effects on the Wnt pathway. We found that Tax could bind to DAPLE and also Dvl2, the cellular partner of DAPLE (Figure 1a). This association was also confirmed to occur endogenously in an ATL cell line, ATL-T (Figure 1b). To further reveal the impact of the association of Tax and DAPLE/Dvl2, we performed reporter assay in Jurkat cells, using Topflash and Fopflash luciferase plasmids, which contain wild-type or mutant TCF/LEF-binding motifs, respectively. Tax and Dvl2 induced canonical Wnt activation, which was greatly enhanced by DAPLE (Figure 1c). As Dvl2 is active upon phosphorylation,[30] we then investigated the effects of Tax and DAPLE on its phosphorylation. We found that DAPLE could induce the phosphorylation of endogenous Dvl2 (Figure 1d, lanes 1 and 6–9), while the amount of Dvl2 was increased when Tax was coexpressed (Figure 1d, lanes 7, 8, 10 and 11). Thus, these results showed that DAPLE and Tax cooperatively enhanced Dvl2 phosphorylation, which might lead to the activation of the canonical Wnt pathway. When we introduced HBZ to this interplay, we found that the activation induced by Tax/Dvl2/DAPLE was dose-dependently suppressed (Figure 1e). In particular, low dose of HBZ was able to abolish the activation by Tax/DAPLE/Dvl2, suggesting a strong suppressive function of HBZ in the canonical Wnt pathway. However, we found that HBZ had no effect on Tax/DAPLE-induced Dvl phosphorylation (data not shown), indicating that Wnt suppression by HBZ might not be a direct consequence of the HBZ–DAPLE interaction. Therefore, although we could not clarify the significance of the interaction between HBZ and DAPLE in the Wnt pathway, we tried to look for other possible targets of HBZ.

HBZ binds to TCF1/LEF1 and impairs DNA-binding ability of LEF1

To find out the mechanism of HBZ-induced canonical Wnt suppression, we first analyzed the effect of HBZ on β-catenin, which is a downstream effector of the Wnt/β-catenin pathway. Surprisingly, both wild-type and constitutively active form of β-catenin-induced hyperactivation of the pathway was greatly suppressed by HBZ (Figure 2a). As constitutively active β-catenin is resistant for the N-terminal phosphorylation and following degradation, we suspected that HBZ-induced canonical Wnt suppression might be independent of β-catenin stability. β-catenin has to cooperate with its nuclear binding partners, TCF/LEF proteins, to induce the canonical Wnt activation. We next focused on the TCF/LEF proteins. We constructed the expression plasmids for LEF1 and TCF1, two members predominantly expressed in T cells,[12,31,32] and found that HBZ colocalized with both proteins in the nucleus (Figure 2b). Co-IP analysis demonstrated the physical interaction between HBZ and LEF1 or HBZ and TCF1 (Figures 2c and d). Deletion of the AD or CD domain of HBZ impaired the interaction, indicating that both domains are implicated in interactions with LEF1/TCF1. These associations were also confirmed in a stable transfectant of HBZ, Jurkat–MycHis–HBZ, in which expression level of HBZ is comparable to ATL cells (Figure 2e and Supplementary Figure S2).

Next, we further analyzed the association of HBZ and LEF1 or TCF1. Because TCF1 and LEF1 are similar in structure and in most cases functionally redundant in T cells,[12,31,32] we chose LEF1 for further analysis. We constructed deletion mutants of LEF1 that lack the N-terminal β-catenin binding domain (ΔβBD), the central context-dependent regulatory domain (ΔCRD) and the C-terminal high-mobility group DNA-binding domain (ΔHMG), respectively. Co-IP experiments indicated that HBZ binds to the conserved DNA-binding domain (HMG) of LEF1 (Figure 2f, lanes 3–5).

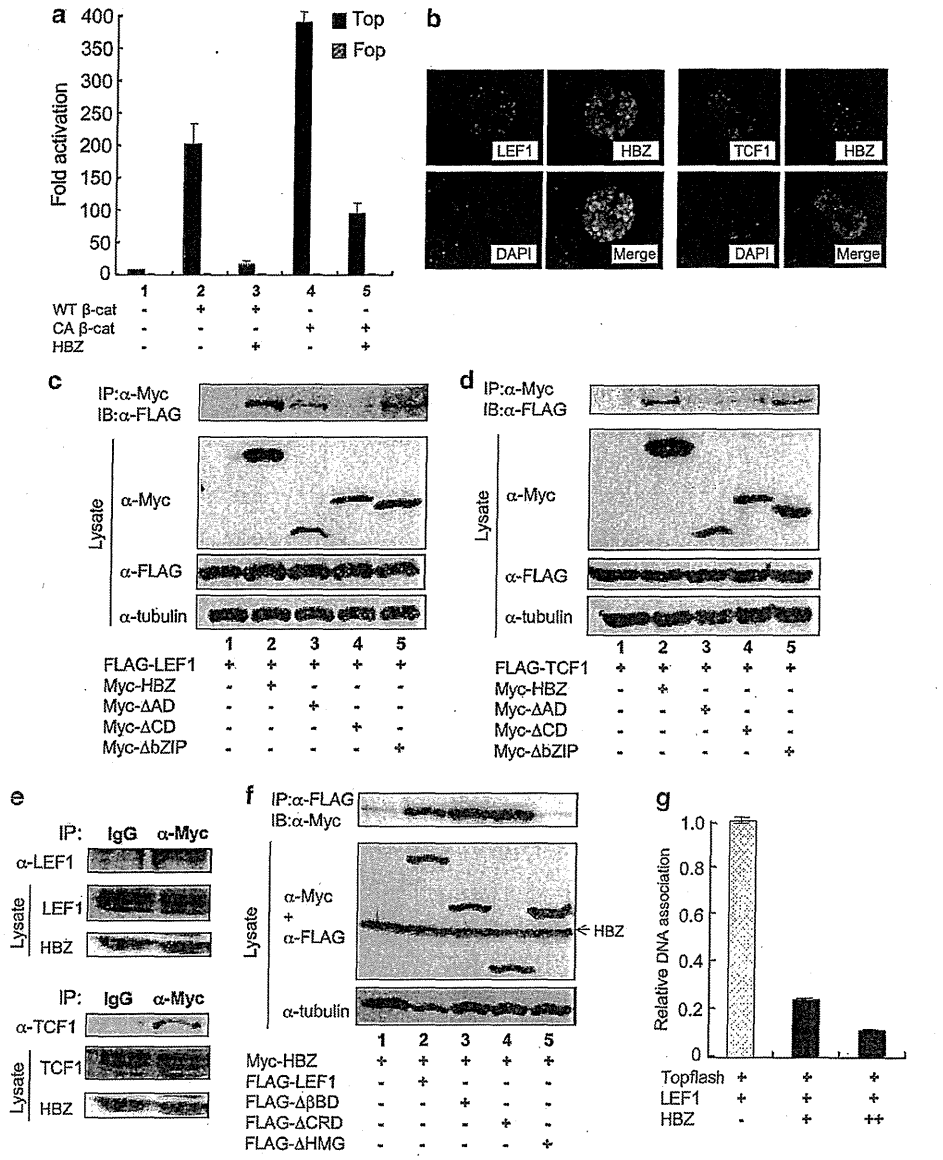

Figure 2. HBZ binds to TCF1/LEF1 and impairs DNA-binding ability of LEF1. (**a**) Effects of HBZ on WT or constitutively active β-catenin-induced canonical Wnt activation. (**b**) Colocalization of HBZ and LEF1 or TCF1 in HeLa cells. (**c**) Co-IP analysis of the interaction of HBZ or its mutants with LEF1 in 293FT cells. (**d**) Co-IP analysis of the interaction of HBZ or its mutants with TCF1 in 293FT cells. (**e**) Endogenous interaction between HBZ and LEF1 or TCF1 in Jurkat–MycHis–HBZ cells. (**f**) Co-IP analysis of the interaction of LEF1 or its mutants with HBZ in 293FT cells. (**g**) Quantitative chromatin immunoprecipitation analysis of the association of LEF1 to specific binding sites in Topflash reporter in the absence (dotted bar) or presence of HBZ (black bars). Result is shown as relative DNA-association capacity.

Speculating that HBZ might interfere with the DNA association of LEF1, we evaluated the effect of HBZ on the DNA-binding ability of LEF1 by quantitative chromatin immunoprecipitation assays. We found that HBZ significantly suppressed the binding of LEF1 to specific TCF/LEF-binding sites (Figure 2g), which accounted for how HBZ could markedly suppress the Wnt/β-catenin pathway.

The canonical Wnt pathway is not activated in HTLV-1-infected cells

It has been reported that active canonical Wnt pathway in T-cell leukemic cell lines, including CEM, Molt4 and SupT1, promotes their proliferation.[33] Because of the strong Wnt-suppressing capacity of HBZ, we assumed that the canonical Wnt pathway might not be activated in HTLV-1-infected cells. We compared the canonical Wnt activity in HTLV-1 noninfected and infected cell lines. In accordance with a previous study,[33] CEM, Molt4 and SupT1 were found to have activated Wnt signaling. Other two HTLV-1 noninfected T-cell lines tested in this study, Jurkat and Hut78, were also active for the canonical Wnt pathway (Figure 3a). On the contrary, the value of Topflash was equivalent to or lower than that of Fopflash in all HTLV-1-infected cell lines (Figure 3a), indicating that the canonical Wnt pathway is not activated in HTLV-1-infected cells. To prove the involvement of HBZ in this nonactivated status, we suppressed HBZ expression in ATL-T. Topflash reporter activity was elevated (Figure 3b), suggesting an increase of canonical Wnt activity. However, no marked but only mild increase of canonical Wnt activity was observed. It is possible

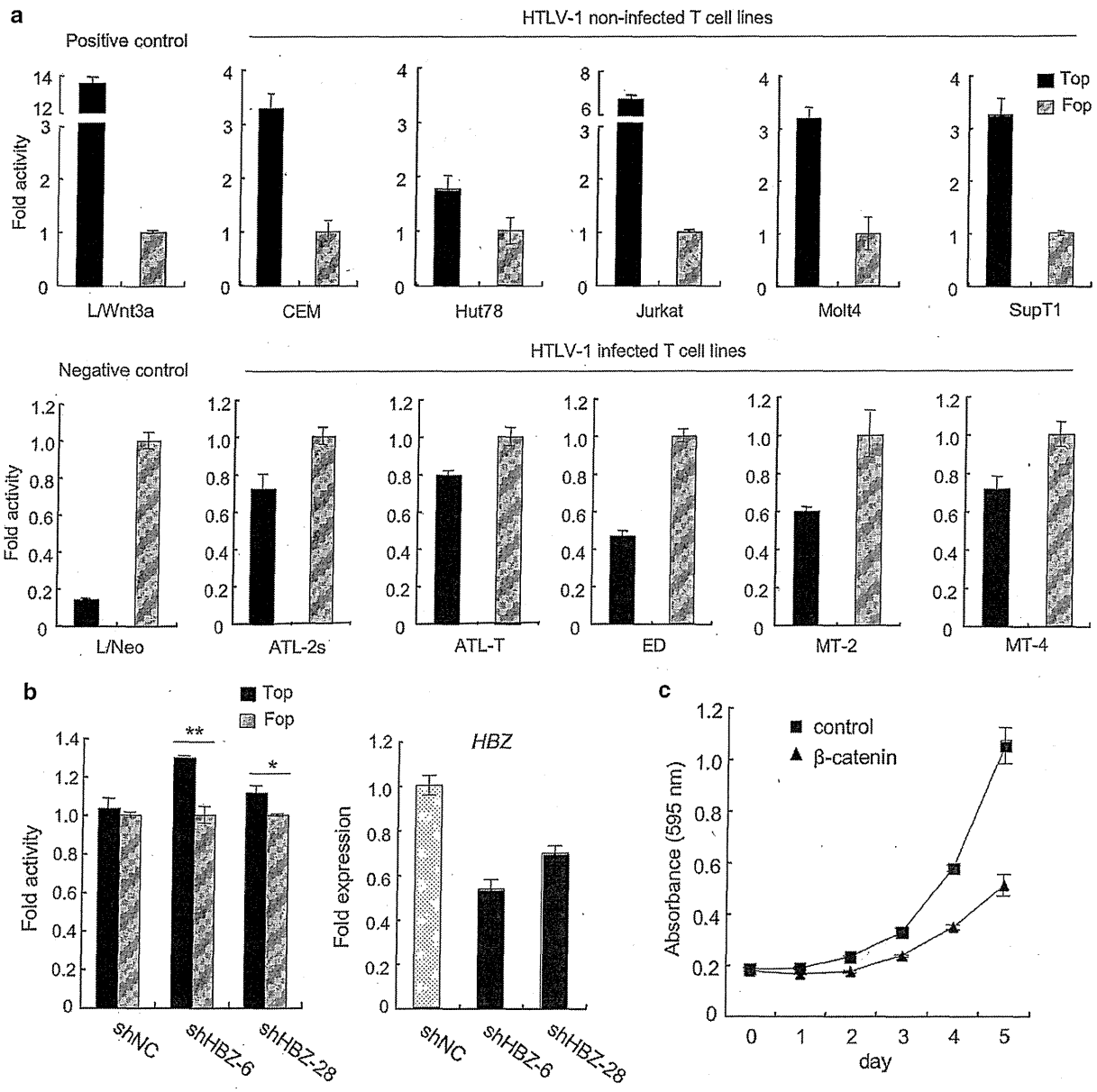

Figure 3. The canonical Wnt pathway is not activated in HTLV-1-infected cells. (**a**) Top/Fop reporter analysis in five HTLV-1-negative T-cell lines (CEM, Hut78, Jurkat, Molt4 and SupT1) and 5 HTLV-1-positive cell lines (ATL-2s, ATL-T, ED, MT-2 and MT-4). Mouse L cell lines expressing Wnt3a (L/Wnt3a) or empty vector (L/Neo) were used as positive or negative control in the reporter assay. Values were shown as fold activity with black bars being Topflash and striped bars being Fopflash. (**b**) Top/Fop reporter analysis in HBZ knockdown (shHBZ-6 and shHBZ-28) or negative control (shNC) ATL-T cells. HBZ knockdown efficiency is confirmed in the right panel. Statistical analysis was performed by Students *t*-test with $^{**}P<0.01$ and $^{*}P<0.05$. (**c**) The 3-(4,5–dimethythiazol–2–yl)-2,5-diphenyl tetrazolium bromide (MTT) assay analysis of β-catenin- (triangle) or mock-transfected (square) ATL-T cells. Transfection was performed by electroporation using Neon (Life Technologies).

that HBZ has strong suppressive ability on the Wnt pathway, so partial knockdown of HBZ might not affect much on the Wnt activity. Indeed, shHBZ-28 induced less-efficient knockdown of HBZ than shHBZ-6, which also resulted in less increase of the Wnt activity. To better understand the physiological importance of the nonactivated canonical Wnt pathway in ATL cells, we enforced activation of the pathway in ATL-T cells by constitutively active β-catenin overexpression. Cell proliferation was decreased (Figure 3c), implying that activation of the Wnt/β-catenin pathway might have suppressive effect on proliferation of ATL cells.

Noncanonical Wnt5a expression is induced by HBZ

It is well established that noncanonical Wnt ligands, such as Wnt5a, usually antagonize the canonical Wnt pathway.[14] Because the latter is not activated in HTLV-1-infected cells, we further investigated the status of the noncanonical Wnt pathway. Quantitative analyses revealed increased expression of Wnt5a in HTLV-1-infected cell lines compared with noninfected ones (Figure 4a). Knockdown of HBZ in HTLV-1-infected cells resulted in downregulation of Wnt5a mRNA expression (Figure 4b), suggesting the involvement of HBZ in the upregulated Wnt5a expression.

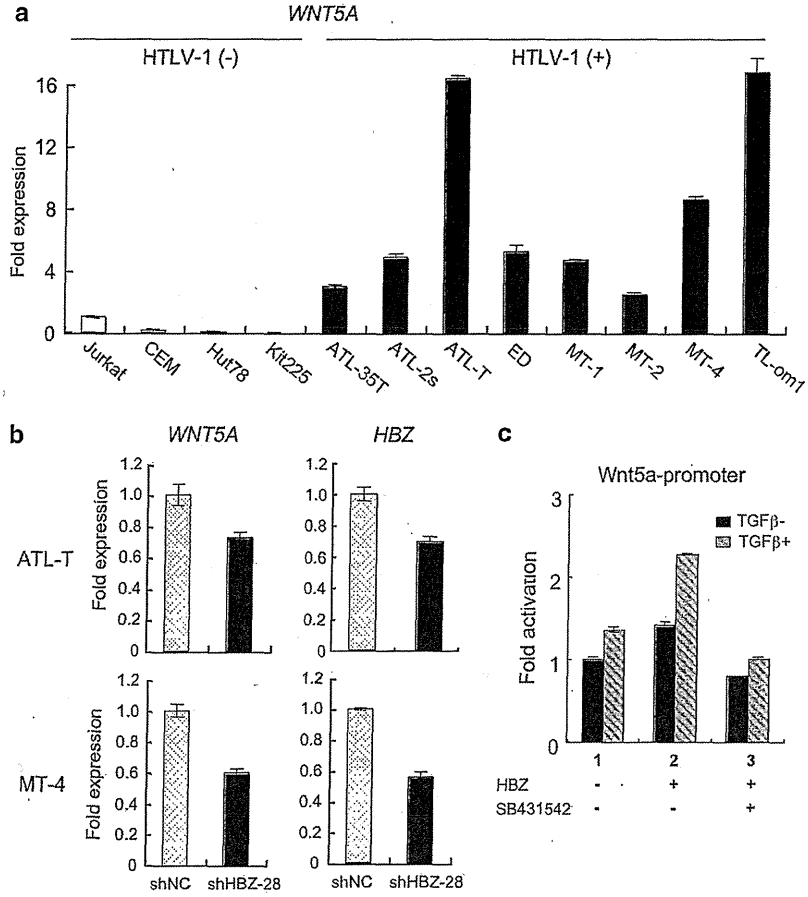

Figure 4. Noncanonical Wnt5a expression is induced by HBZ. (**a**) Quantitative analysis of *WNT5A* mRNA in HTLV-1-negative (open bars) and -positive cell lines (black bars) by real-time PCR. (**b**) Quantitative comparison of *WNT5A* mRNA levels between HBZ knockdown (shHBZ-28, black bars) and negative control (shNC, dotted bars) cells in one ATL cell line (ATL-T) and one HTLV-1-transformed cell line (MT-4) by real-time PCR. Left panel shows expression of *WNT5A* mRNA, whereas right panel indicates the efficiency of HBZ knockdown. (**c**) Reporter analysis in HepG2 cells to assess the effect of HBZ on Wnt5a promoter activity, in the absence (black bars) or presence (striped bars) of TGF-β. SB431542 (5 μM) is a specific inhibitor for TGF-β receptor.

It has been reported that TGF-β can induce Wnt5a expression.[34,35] Meanwhile, according to our previous report, HBZ activates the TGF-β signaling pathway.[36] These reports suggest that HBZ-induced Wnt5a expression is associated with the TGF-β signaling pathway. We cloned a 2-kb fragment of the Wnt5a promoter region into the pGL4.10 reporter plasmid and performed reporter assay in a TGF-β-responsive cell line, HepG2. We found that HBZ enhanced transcription from the Wnt5a promoter, which was further enhanced by TGF-β (Figure 4c, lanes 1 and 2). An inhibitor of the TGF-β receptor, SB431542,[36] suppressed the activation of Wnt5a promoter by HBZ, thereby indicating that the TGF-β pathway is implicated in this activation (Figure 4c, lane 3). These results suggest that HBZ can induce Wnt5a transcription through activating its promoter via the TGF-β pathway.

Wnt5a supports proliferation and migration of HTLV-1-infected cells

To clarify the physiological significance of upregulated Wnt5a expression in HTLV-1-positive cells, we knocked down Wnt5a by short hairpin RNA (shRNA) in several cell lines, including ATL-T, MT-2 and MT-4. Suppressing Wnt5a expression impaired cell proliferation (Figure 5a). Recent studies have shown that Wnt5a is involved in cancer metastasis,[37,38] so we further analyzed cell migration. We found that knockdown of Wnt5a impaired cell migration using a trans-well T-cell migration assay (Figure 5b). As Wnt5a is a secreted ligand, we next studied effect of an antibody to Wnt5a on migration of HTLV-1-infected cell lines. Anti-Wnt5a antibody suppressed migrating ability of ATL-T and MT-2 cells (Figure 5c). In addition, to confirm the specificity of the shRNA and anti-Wnt5a antibody used in ATL cells, we performed similar experiments in an HTLV-1-negative T-cell line, CEM, in which Wnt5a is undetectable by real-time PCR. As expected, neither cell proliferation nor migration was affected by inhibition of Wnt5a (Supplementary Figure S3). Collectively, these results demonstrated a supporting role of Wnt5a in the proliferation and migration of ATL cells.

DISCUSSION

Dysregulation of the Wnt pathways has been implicated in viral transformation,[15–19] and several viral proteins are known to interact with the key cellular factors of this pathway. The hepatitis B viral X protein binds to adenomatous polyposis coli,[15] and the nonstructural 5A protein of hepatitis C virus targets the interaction between β-catenin and GSK-3β.[16] Both hepatitis virus-encoded proteins induce the nuclear accumulation of β-catenin, which is associated with the pathogenesis of hepatocellular carcinoma. Similarly, the Kaposi's sarcoma-associated herpesvirus latency-associated nuclear antigen interacts with GSK-3β and

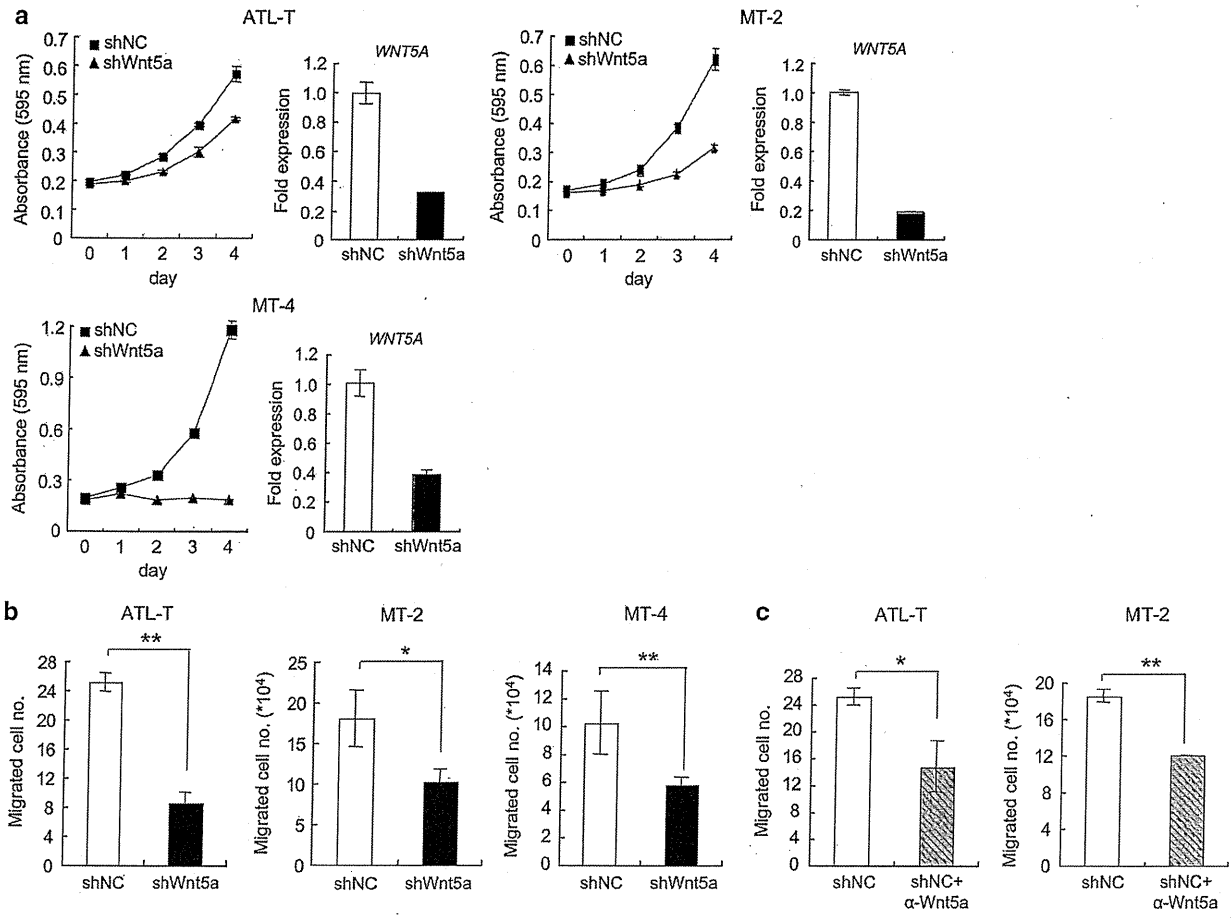

Figure 5. Wnt5a supports proliferation and migration of HTLV-1-infected cells. (**a**) MTT results in Wnt5a knockdown (shWnt5a, triangle) and negative control (shNC, square) of ATL-T, MT-2 and MT-4 cells. Wnt5a knockdown was confirmed by real-time PCR and shown in the right panel of each cell line (black bar for knockdown and open bar for negative control). (**b**) Migrating ability analysis of Wnt5a knockdown (shWnt5a, black bar) and negative control (shNC, open bar) of ATL-T, MT-2 and MT-4 cells. Migrated ATL-T cells that attached to the membrane were stained and counted for at least five random fields under a microscope to obtain an average number. Migrated MT-2 and MT-4 cells were collected and total cell numbers were counted. Values are shown as average migrated cell numbers of three independent wells. Statistical analysis was performed with Student's *t*-test with $^{**}P<0.01$ and $^{*}P<0.05$. (**c**) To mimic the knockdown effect, negative control cells for Wnt5a knockdown of ATL-T and MT-2 were treated with 0.2 μg/ml of anti-Wnt5a antibody (R&D systems, Minneapolis, MN, USA) and migrating ability was measured.

stabilizes β-catenin.[17] To our knowledge, all reported instances of virus-induced Wnt dysregulation were the activation of the canonical pathway due to the stabilization of β-catenin. On the contrary, here we demonstrate that HTLV-1 employs a unique mechanism to inhibit the canonical Wnt pathway. The viral protein HBZ is able to potently suppress canonical Wnt activation by targeting downstream of β-catenin. Because the canonical and noncanonical pathways are mutually antagonistic, it is possible that canonical Wnt suppression by HBZ facilitates noncanonical Wnt activation, for proliferation and migration of ATL cells.

It has been reported that TCF1 and LEF1 are predominantly expressed in T cells.[12,31,32] Targeted inhibition of LEF1/TCF1 by HBZ and resulting inactivation of the target gene transcription is an efficient way to block the canonical Wnt pathway in T cells. In addition, HBZ has an alternate mechanism for the suppression of the canonical Wnt pathway: it is able to induce transcription of the noncanonical Wnt5a, which antagonizes the canonical Wnt pathway.[14] Although the canonical Wnt pathway is crucial for T-cell development,[12,13] its functional role in mature T cells is barely understood so far. A recent study has shown that β-catenin is a negative regulator of peripheral T-cell activation.[39] It is possible that HBZ achieves canonical Wnt suppression in order to promote cellular proliferation in the periphery. These multiple strategies by HBZ could restrict HTLV-1-infected cells to inactive canonical Wnt pathway and allow peripheral T cells to be activated.

Besides its contribution to canonical Wnt suppression as an antagonist, HBZ-induced Wnt5a expression has another significance. Although Wnt5a has been regarded as a tumor-suppressor gene in various studies,[14] accumulating evidence suggests its oncogenic capacity. Overexpression of Wnt5a in tumor cells has been a predictor of poor prognosis for several cancers.[40–43] Moreover, Wnt5a is also involved in promoting cancer invasion and metastasis,[37,38,44–46] implying that Wnt5a contributes to tumor progression. This study showed the oncogenic role of Wnt5a in ATL and its involvement in ATL cell expansion, based on our findings that knockdown of Wnt5a inhibits both cellular proliferation and migration. Indeed, through analyzing the microarray data (available in the public Gene Expression Omnibus database) provided by the project named Joint Study on Prognostic Factors of ATL Development,[47] we found that the transcription level of Wnt5a was significantly elevated in ATL cases (Supplementary Figure S4a), which strongly supports our conclusion.

It is of great interest to notice that HBZ counteracts Tax in many signaling pathways, such as NF-κB, CREB and TGF-β.[26–28,36] Tax is a

potent activator of both the canonical and noncanonical NF-κB pathways and has an important role in cellular transformation *in vitro*.[6,48] However, recently it has been reported that cellular senescence is induced by Tax-mediated NF-κB activation.[49] HBZ inactivates p65 and inhibits selectively the canonical NF-κB pathway,[26] helping cells to evade senescence and supporting cell proliferation.[49] This suggests a possible role of HBZ to counteract against Tax and thus bypass underlying negative effects by Tax in various signaling pathways. In this study, we found that Tax is actually an activator of the Wnt/β-catenin pathway through forming complex with DAPLE and Dvl, whereas HBZ represses the pathway downstream of β-catenin, suggesting that HBZ can avoid possible negative effects of Tax on this pathway, as in the interplay of HBZ and Tax in NF-κB regulation. Indeed, it has been reported that the canonical Wnt pathway was activated in an HTLV-1-transformed cell line C8166 and *ex vivo* cultured cells from one ATL patient.[50] Because C8166 expresses much higher amount of Tax protein than other HTLV-1-transformed or ATL cell lines,[51] and primary HTLV-1-infected cells start expressing Tax immediately after being subjected to *ex vivo* culture,[52] regulation of the Wnt pathway by Tax might be dominant in such setting. We speculate that the Wnt signaling cascades in HTLV-1-infected cells are dysregulated in different ways under various conditions. Because HBZ harbors a strong suppressive ability for the canonical Wnt pathway and its expression level is higher than that of Tax in fresh ATL cells,[53] we hypothesize that the canonical Wnt activity is suppressed by HBZ in fully transformed ATL cells *in vivo*. In support of our hypothesis, *AXIN2*, the most well-characterized canonical Wnt target gene,[13,54] is downregulated in ATL patients compared with normal controls (Supplementary Figure S4b), indicating the inactive state of the canonical Wnt pathway. Nevertheless, additional investigation will be needed to understand how HBZ and Tax regulate the status of the Wnt pathways throughout the leukemogenic processes of ATL.

In summary, we show that HBZ is able to suppress the canonical Wnt pathway by multiple strategies, such as interaction with LEF1/TCF1 and induction of Wnt5a. Importantly, we demonstrate that Wnt5a, induced by HBZ in ATL cells, promotes both cellular proliferation and migration. This study on the dysregulation of the Wnt pathways by HBZ may unveil new molecular processes of oncogenesis by HTLV-1 and contribute to the development of novel therapeutic strategies.

MATERIALS AND METHODS

Yeast two-hybrid screen

A yeast two-hybrid screen was performed by Hybrigenics (http:/www.hybrigenics.com) on a random-primed Leukocytes and Activated Mononuclear Cells cDNA library using full length of spliced form HBZ as the bait.

Cell culture

ATL-35T, ATL-2s, ATL-T, ED, MT-1, MT-2 and MT-4 are HTLV-1-infected T-cell lines. Jurkat, CEM, Hut78, Molt4, SupT1 and Kit225 are HTLV-1-negative T-cell lines. All T-cell lines were cultured in RPMI-1640 supplemented with 10% fetal calf serum and antibiotics (penicillin and streptomycin). IL-2-dependent Kit225 was cultured with 85 μ/ml IL-2 in the medium. HEK293FT, HeLa, HepG2, L/Wnt3a and L/Neo were cultured in DMEM supplemented with 10% fetal calf serum and antibiotics. L/Wnt3a and L/Neo were stable transfectants of mouse L fibroblast cell line used as positive and negative control in our Top/Fop reporter assay.[55] Jurkat–MycHis–HBZ is established by overexpressing MycHis–HBZ and subsequent G418 selection and is maintained in normal RPMI-1640 medium supplemented with 1000 μg/ml G418.

Plasmids

Coding sequence of DAPLE was amplified using PCR using Herculase II Fusion DNA polymerase (Agilent Technologies, Inc., Santa Clara, CA, USA) and cloned into pCMV-Tag2 (Agilent Technologies, Inc.) to fuse FLAG tags in the N terminus. Expression vectors for HBZ and it mutants, Tax, SuperTopflash, SuperFopflash, pcDNA3/myc-Dvl2, pPolIII-Renilla, pEF-wtbcat and pEF-mmbcat, were described previously.[26,56–58] Expression vectors for LEF1 and its mutants were generated by PCR amplification from cDNA of SupT1 and then subcloned into pCAG-FLAG vector to fuse FLAG tags in the N terminals.[59] Expression vectors for TCF1 were generated by PCR amplification from cDNA of Jurkat and then subcloned into pCAG-FLAG or pCAG-HA vector to fuse FLAG or HA tag in the N terminals.[59]

Luciferase reporter assay

Generally, 2×10^5 cells per well were seeded in a 12-well plate and transfected with indicated combinations of plasmids using Lipofectamine LTX reagent (Life technologies, Carlsbad, CA, USA). Twenty-four hours later, cells were harvested and luciferase activities were measured using Dual-Luciferase Reporter Assay System (Promega, Madison, WI, USA) according to the manufacturer's instructions. All luciferase values were normalized with the activity of Renilla luciferase and represented as the mean of a triplicate set of experiments. CEM, Hut78, Molt4 and SupT1 were transfected by electroporation using Neon (Life technologies).

Knockdown

Knockdown of HBZ in HTLV-1-infected cells was performed with a lentivirus-based shRNA system, as described previously.[8] Knockdown of Wnt5a was performed with a lentiviral vector pLKO.1-based shRNA system (Open Biosystems, Lafayette, CO, USA). shRNA sequence specifically targeting exon 5 of Wnt5a was 5′-CGTGGACCAGTTTGTGTGCAACTCGAGTTGCACACA AACTGGTCCACG-3′.

Quantitative real-time PCR

Total RNA was isolated using TRIzol Reagent (Life technologies) according to the manufacturer's instructions. An amount of 1 μg of isolated total RNA was used to synthesize cDNA using SuperScript III reverse transcriptase (Life technologies). cDNA product was quantified with Power SYBR Green PCR Master Mix and StepOnePlus Real Time PCR System (Life technologies). Endogenous *ACTB* mRNA was quantified to normalize the amount of cDNA load. Primer sequences from 5′ to 3′ are: TAAACTTACCTAGACGG CGG and CTGCCGATCACGATGCGTTT for *HBZ*; CATCCTCATGAACCTGCAC AAC and AAGCGGCTGTTGACCTGTAC for *WNT5A*; and AGGCCAACCGCGAG AAGATG and CTATCCCTGTACGCCTCTGG for *ACTB*.

Lentiviral transduction

For packaging of the lentiviral vectors, 3×10^6 293FT cells were seeded in a 10-cm dish and transfected with 7.5 μg of pVSV-G, 15 μg of pCMV-Δ8/9 (kindly provided by Dr Miyoshi H; RIKEN, Tsukuba, Japan) and 15 μg of transfer vector using TransIT-LT1 reagent (Mirus, Madison, WI, USA). Virus was harvested by collecting supernatant at both 48 and 72 h and concentrated by centrifugation at 25 000 *g* for 2 h at 4 °C.

3-(4,5–dimethythiazol–2–yl)-2,5-diphenyl tetrazolium bromide assay

Cells were seeded in 96-well plates and at indicated time points, 10 μl of 3-(4,5–dimethythiazol–2–yl)-2,5-diphenyl tetrazolium bromide solution was added. Cells were incubated at 37 °C for 2 h and then lysed by 100 μl of lysis buffer (4% Triton X-100 and 0.14% HCl in 2-propanol). Absorbance at 595 nm was measured by using a Microplate Reader (BERTHOLD TECHNOLOGIES GmbH & Co. KG, Bad Wildbad, Germany).

Co-immunoprecipitation

Co-IP in 293FT cells was performed as previously reported.[26] For the endogenous interaction between Tax and Dvl2 or DAPLE, ATL-T total cell lysate was incubated with anti-Tax (clone MI73)[60] or normal mouse IgG (Santa Cruz Biotechnology, Santa Cruz, CA, USA) overnight at 4 °C, and following procedures were same as in 293FT. For the endogenous interaction between HBZ and LEF1 or TCF1, nuclear lysate of Jurkat–Myc–HBZ was extracted by nuclear complex Co-IP kit (Active Motif, Carlsbad, CA, USA) and incubated with anti-Myc (clone 4A6, Millipore, Billerica, MA, USA) or normal mouse IgG overnight at 4 °C. Following procedures were same as in 293FT. Antibodies used were as follows: anti-FLAG M2 (Sigma-Aldrich, St Louis, MO, USA), anti-Myc (clone 9E10, Sigma-Aldrich), anti-Myc (clone 4A6, Millipore), anti-Tax (clone MI73),[60]

anti-Dvl2 (Cell Signaling Technology, Danvers, MA, USA) and anti-α-tubulin (clone DM1A, Sigma-Aldrich). Horseradish peroxidase-conjugated anti-mouse IgG was purchased from Sigma-Aldrich and horseradish peroxidase-conjugated anti-rabbit IgG was purchased from Cell Signaling Technology. Polyclonal antibody for DAPLE was generated by MBL International (Way Woburn, MA, USA).

Immunostaining

HeLa cells were transfected with Myc–HBZ and FLAG-LEF1 or HA-TCF1, respectively. After 48 h, cells were fixed with 4% formaldehyde, permeabilized with 0.1% Triton X-100 and blocked with 5% bovine serum albumin. Antibody incubation was performed at room temperature for 1 h using anti-Myc-FITC and anti-FLAG-Cy3 (Sigma-Aldrich) or anti-HA-Alexa488 (Cell Signaling Technology) and anti-Myc-Cy3 (Sigma-Aldrich). Cells were mounted with Vectashield mounting medium (Vector Laboratories, Burlingame, CA, USA) and observed under a Leica confocal microscope (Leica Microsystems GmbH, Wetzlar, Germany).

Quantitative chromatin immunoprecipitation assay

Chromatin immunoprecipitation assay was performed as previously described.[61] Briefly, 293FT cells were seeded in a 10-cm dish and transfected with 1 μg of SuperTopflash and 1 μg of FLAG-LEF1, with or without 2 or 4 μg of Myc–HBZ. After 48 h, cells were fixed and subjected to immunoprecipitation with anti-FLAG (M2, Sigma-Aldrich) or normal mouse IgG (Santa Cruz Biotechnology) overnight at 4 °C. Precipitated DNA was purified and subjected to real-time PCR amplification. Primer sequences flanking the specific TCF/LEF-binding sites were 5′-TAGGCTG TCCCCAGTGCAAG-3′ and 5′-TGCCAAGCTGGAATTCGAGC-3′.

Trans-well migration assay

A 24-well migration plate (BD Biosicences, San Jose, CA, USA) with 8 μm insert pore size was used and all the procedures were performed following the manufacturer's instructions. Generally, 2×10^5 cells in RPMI-1640 with 1% fetal bovine serum were seeded onto the inserts and allowed for migration toward 10% fetal bovine serum containing medium within 24 h. In the case of ATL-T, migrated cells attached to the basolateral side of the membrane and were stained with Diff Quik (Sysmex, Kobe, Japan) and counted under a microscope. In the case of MT-2 and MT-4, migrated cells were collected and counted by an automated cell counter, Countess (Life technologies). The number of migrated cells were calculated as an average of three independent experiments.

CONFLICT OF INTEREST

The authors declare no conflict of interest.

ACKNOWLEDGEMENTS

We thank H Miyoshi for providing lentiviral packaging vectors and L Kingsbury for proofreading of this manuscript. This work was supported by a Grant-in-aid for Scientific Research from the Ministry of Education, Science, Sports, and Culture of Japan to MM, and a grant from the Takeda Science Foundation to JY.

REFERENCES

1 Poiesz BJ, Ruscetti FW, Gazdar AF, Bunn PA, Minna JD, Gallo RC. Detection and isolation of type C retrovirus particles from fresh and cultured lymphocytes of a patient with cutaneous T-cell lymphoma. *Proc Natl Acad Sci USA* 1980; **77**: 7415–7419.
2 Hinuma Y, Nagata K, Hanaoka M, Nakai M, Matsumoto T, Kinoshita KI *et al.* Adult T-cell leukemia: antigen in an ATL cell line and detection of antibodies to the antigen in human sera. *Proc Natl Acad Sci USA* 1981; **78**: 6476–6480.
3 Takatsuki K. Discovery of adult T-cell leukemia. *Retrovirology* 2005; **2**: 16.
4 Gallo RC. The discovery of the first human retrovirus: HTLV-1 and HTLV-2. *Retrovirology* 2005; **2**: 17.
5 Matsuoka M, Jeang KT. Human T-cell leukaemia virus type 1 (HTLV-1) infectivity and cellular transformation. *Nat Rev Cancer* 2007; **7**: 270–280.
6 Grassmann R, Aboud M, Jeang KT. Molecular mechanisms of cellular transformation by HTLV-1 Tax. *Oncogene* 2005; **24**: 5976–5985.
7 Franchini G, Fukumoto R, Fullen JR. T-cell control by human T-cell leukemia/lymphoma virus type 1. *Int J Hematol* 2003; **78**: 280–296.
8 Satou Y, Yasunaga J, Yoshida M, Matsuoka M. HTLV-I basic leucine zipper factor gene mRNA supports proliferation of adult T cell leukemia cells. *Proc Natl Acad Sci USA* 2006; **103**: 720–725.
9 Arnold J, Zimmerman B, Li M, Lairmore MD, Green PL. Human T-cell leukemia virus type-1 antisense-encoded gene, Hbz, promotes T-lymphocyte proliferation. *Blood* 2008; **112**: 3788–3797.
10 Satou Y, Yasunaga J, Zhao T, Yoshida M, Miyazato P, Takai K *et al.* HTLV-1 bZIP factor induces T-cell lymphoma and systemic inflammation in vivo. *PLoS Pathog* 2011; **7**: e1001274.
11 MacDonald BT, Tamai K, He X. Wnt/beta-catenin signaling: components, mechanisms, and diseases. *Dev Cell* 2009; **17**: 9–26.
12 Staal FJ, Clevers HC. WNT signalling and haematopoiesis: a WNT-WNT situation. *Nat Rev Immunol* 2005; **5**: 21–30.
13 Staal FJ, Luis TC, Tiemessen MM. WNT signalling in the immune system: WNT is spreading its wings. *Nat Rev Immunol* 2008; **8**: 581–593.
14 McDonald SL, Silver A. The opposing roles of Wnt-5a in cancer. *Br J Cancer* 2009; **101**: 209–214.
15 Cha MY, Kim CM, Park YM, Ryu WS. Hepatitis B virus X protein is essential for the activation of Wnt/beta-catenin signaling in hepatoma cells. *Hepatology* 2004; **39**: 1683–1693.
16 Street A, Macdonald A, McCormick C, Harris M. Hepatitis C virus NS5A-mediated activation of phosphoinositide 3-kinase results in stabilization of cellular beta-catenin and stimulation of beta-catenin-responsive transcription. *J Virol* 2005; **79**: 5006–5016.
17 Fujimuro M, Wu FY, ApRhys C, Kajumbula H, Young DB, Hayward GS *et al.* A novel viral mechanism for dysregulation of beta-catenin in Kaposi's sarcoma-associated herpesvirus latency. *Nat Med* 2003; **9**: 300–306.
18 Shackelford J, Maier C, Pagano JS. Epstein–Barr virus activates beta-catenin in type III latently infected B lymphocyte lines: association with deubiquitinating enzymes. *Proc Natl Acad Sci USA* 2003; **100**: 15572–15576.
19 Uren A, Fallen S, Yuan H, Usubutun A, Kucukali T, Schlegel R *et al.* Activation of the canonical Wnt pathway during genital keratinocyte transformation: a model for cervical cancer progression. *Cancer Res* 2005; **65**: 6199–6206.
20 Muller-Tidow C, Steffen B, Cauvet T, Tickenbrock L, Ji P, Diederichs S *et al.* Translocation products in acute myeloid leukemia activate the Wnt signaling pathway in hematopoietic cells. *Mol Cell Biol* 2004; **24**: 2890–2904.
21 Lu D, Zhao Y, Tawatao R, Cottam HB, Sen M, Leoni LM *et al.* Activation of the Wnt signaling pathway in chronic lymphocytic leukemia. *Proc Natl Acad Sci USA* 2004; **101**: 3118–3123.
22 McWhirter JR, Neuteboom ST, Wancewicz EV, Monia BP, Downing JR, Murre C. Oncogenic homeodomain transcription factor E2A-Pbx1 activates a novel WNT gene in pre-B acute lymphoblastoid leukemia. *Proc Natl Acad Sci USA* 1999; **96**: 11464–11469.
23 Jamieson CH, Ailles LE, Dylla SJ, Muijtjens M, Jones C, Zehnder JL *et al.* Granulocyte-macrophage progenitors as candidate leukemic stem cells in blast-crisis CML. *N Engl J Med* 2004; **351**: 657–667.
24 Hagiya K, Yasunaga J, Satou Y, Ohshima K, Matsuoka M. ATF3 an HTLV-1 bZip factor binding protein, promotes proliferation of adult T-cell leukemia cells. *Retrovirology* 2011; **8**: 19.
25 Oshita A, Kishida S, Kobayashi H, Michiue T, Asahara T, Asashima M *et al.* Identification and characterization of a novel Dvl-binding protein that suppresses Wnt signalling pathway. *Genes Cells* 2003; **8**: 1005–1017.
26 Zhao T, Yasunaga J, Satou Y, Nakao M, Takahashi M, Fujii M *et al.* Human T-cell leukemia virus type 1 bZIP factor selectively suppresses the classical pathway of NF-kappaB. *Blood* 2009; **113**: 2755–2764.
27 Gaudray G, Gachon F, Basbous J, Biard-Piechaczyk M, Devaux C, Mesnard JM. The complementary strand of the human T-cell leukemia virus type 1 RNA genome encodes a bZIP transcription factor that down-regulates viral transcription. *J Virol* 2002; **76**: 12813–12822.
28 Lemasson I, Lewis MR, Polakowski N, Hivin P, Cavanagh MH, Thebault S *et al.* Human T-cell leukemia virus type 1 (HTLV-1) bZIP protein interacts with the cellular transcription factor CREB to inhibit HTLV-1 transcription. *J Virol* 2007; **81**: 1543–1553.
29 Clerc I, Polakowski N, Andre-Arpin C, Cook P, Barbeau B, Mesnard JM *et al.* An interaction between the human T cell leukemia virus type 1 basic leucine zipper factor (HBZ) and the KIX domain of p300/CBP contributes to the down-regulation of tax-dependent viral transcription by HBZ. *J Biol Chem* 2008; **283**: 23903–23913.
30 Yanagawa S, van Leeuwen F, Wodarz A, Klingensmith J, Nusse R. The dishevelled protein is modified by wingless signaling in Drosophila. *Genes Dev* 1995; **9**: 1087–1097.
31 van de Wetering M, Oosterwegel M, Dooijes D, Clevers H. Identification and cloning of TCF-1, a T lymphocyte-specific transcription factor containing a sequence-specific HMG box. *EMBO J* 1991; **10**: 123–132.
32 Travis A, Amsterdam A, Belanger C, Grosschedl R. LEF-1, a gene encoding a lymphoid-specific protein with an HMG domain, regulates T-cell receptor alpha enhancer function (corrected). *Genes Dev* 1991; **5**: 880–894.

33 Groen RW, Oud ME, Schilder-Tol EJ, Overdijk MB, ten Berge D, Nusse R *et al.* Illegitimate WNT pathway activation by beta-catenin mutation or autocrine stimulation in T-cell malignancies. *Cancer Res* 2008; **68**: 6969–6977.
34 Roarty K, Serra R. Wnt5a is required for proper mammary gland development and TGF-beta-mediated inhibition of ductal growth. *Development* 2007; **134**: 3929–3939.
35 Katoh M. Transcriptional mechanisms of WNT5A based on NF-kappaB, Hedgehog, TGFbeta, and Notch signaling cascades. *Int J Mol Med* 2009; **23**: 763–769.
36 Zhao T, Satou Y, Sugata K, Miyazato P, Green PL, Imamura T *et al.* HTLV-1 bZIP factor enhances TGF-beta signaling through p300 coactivator. *Blood* 2011; **118**: 1865–1876.
37 Weeraratna AT, Jiang Y, Hostetter G, Rosenblatt K, Duray P, Bittner M *et al.* Wnt5a signaling directly affects cell motility and invasion of metastatic melanoma. *Cancer Cell* 2002; **1**: 279–288.
38 Dissanayake SK, Wade M, Johnson CE, O'Connell MP, Leotlela PD, French AD *et al.* The Wnt5A/protein kinase C pathway mediates motility in melanoma cells via the inhibition of metastasis suppressors and initiation of an epithelial to mesenchymal transition. *J Biol Chem* 2007; **282**: 17259–17271.
39 Driessens G, Zheng Y, Locke F, Cannon JL, Gounari F, Gajewski TF. Beta-catenin inhibits T cell activation by selective interference with linker for activation of T cells-phospholipase C-gamma1 phosphorylation. *J Immunol* 2011; **186**: 784–790.
40 Badiglian Filho L, Oshima CT, De Oliveira Lima F, De Oliveira Costa H, De Sousa Damiao R, Gomes TS *et al.* Canonical and noncanonical Wnt pathway: a comparison among normal ovary, benign ovarian tumor and ovarian cancer. *Oncol Rep* 2009; **21**: 313–320.
41 Kageshita T, Hamby CV, Ishihara T, Matsumoto K, Saida T, Ono T. Loss of beta-catenin expression associated with disease progression in malignant melanoma. *Br J Dermatol* 2001; **145**: 210–216.
42 Bachmann IM, Straume O, Puntervoll HE, Kalvenes MB, Akslen LA. Importance of P-cadherin, beta-catenin, and Wnt5a/frizzled for progression of melanocytic tumors and prognosis in cutaneous melanoma. *Clin Cancer Res* 2005; **11**: 8606–8614.
43 Da Forno PD, Pringle JH, Hutchinson P, Osborn J, Huang Q, Potter L *et al.* WNT5A expression increases during melanoma progression and correlates with outcome. *Clin Cancer Res* 2008; **14**: 5825–5832.
44 Klemm F, Bleckmann A, Siam L, Chuang HN, Rietkotter E, Behme D *et al.* Beta-catenin-independent WNT signaling in basal-like breast cancer and brain metastasis. *Carcinogenesis* 2011; **32**: 434–442.
45 Yamamoto H, Oue N, Sato A, Hasegawa Y, Matsubara A, Yasui W *et al.* Wnt5a signaling is involved in the aggressiveness of prostate cancer and expression of metalloproteinase. *Oncogene* 2010; **29**: 2036–2046.
46 Sukarawan W, Simmons D, Suggs C, Long K, Wright JT. WNT5A expression in ameloblastoma and its roles in regulating enamel epithelium tumorigenic behaviors. *Am J Pathol* 2010; **176**: 461–471.
47 Yamagishi M, Nakano K, Miyake A, Yamochi T, Kagami Y, Tsutsumi A *et al.* Polycomb-mediated loss of miR-31 activates NIK-dependent NF-kappaB pathway in adult T cell leukemia and other cancers. *Cancer Cell* 2012; **21**: 121–135.
48 Peloponese Jr JM, Yasunaga J, Kinjo T, Watashi K, Jeang KT. Peptidylproline cis-trans-isomerase Pin1 interacts with human T-cell leukemia virus type 1 tax and modulates its activation of NF-kappaB. *J Virol* 2009; **83**: 3238–3248.
49 Zhi H, Yang L, Kuo YL, Ho YK, Shih HM, Giam CZ. NF-kappaB hyper-activation by HTLV-1 tax induces cellular senescence, but can be alleviated by the viral anti-sense protein HBZ. *PLoS Pathog* 2011; **7**: e1002025.
50 Pise-Masison CA, Radonovich M, Dohoney K, Morris JC, O'Mahony D, Lee MJ *et al.* Gene expression profiling of ATL patients: compilation of disease-related genes and evidence for TCF4 involvement in BIRC5 gene expression and cell viability. *Blood* 2009; **113**: 4016–4026.
51 Kuo YL, Giam CZ. Activation of the anaphase promoting complex by HTLV-1 tax leads to senescence. *EMBO J* 2006; **25**: 1741–1752.
52 Hanon E, Hall S, Taylor GP, Saito M, Davis R, Tanaka Y *et al.* Abundant tax protein expression in CD4+ T cells infected with human T-cell lymphotropic virus type I (HTLV-I) is prevented by cytotoxic T lymphocytes. *Blood* 2000; **95**: 1386–1392.
53 Saito M, Matsuzaki T, Satou Y, Yasunaga J, Saito K, Arimura K *et al. In vivo* expression of the HBZ gene of HTLV-1 correlates with proviral load, inflammatory markers and disease severity in HTLV-1 associated myelopathy/tropical spastic paraparesis (HAM/TSP). *Retrovirology* 2009; **6**: 19.
54 Jho EH, Zhang T, Domon C, Joo CK, Freund JN, Costantini F. Wnt/beta-catenin/Tcf signaling induces the transcription of axin2, a negative regulator of the signaling pathway. *Mol Cell Biol* 2002; **22**: 1172–1183.
55 Shibamoto S, Higano K, Takada R, Ito F, Takeichi M, Takada S. Cytoskeletal reorganization by soluble Wnt-3a protein signalling. *Genes Cells* 1998; **3**: 659–670.
56 Lee JS, Ishimoto A, Yanagawa S. Characterization of mouse dishevelled (Dvl) proteins in Wnt/Wingless signaling pathway. *J Biol Chem* 1999; **274**: 21464–21470.
57 Yanagawa S, Lee JS, Matsuda Y, Ishimoto A. Biochemical characterization of the *Drosophila* axin protein. *FEBS Lett* 2000; **474**: 189–194.
58 Tezuka N, Brown AM, Yanagawa S. GRB10 binds to LRP6, the Wnt co-receptor and inhibits canonical Wnt signaling pathway. *Biochem Biophys Res Commun* 2007; **356**: 648–654.
59 Watashi K, Khan M, Yedavalli VR, Yeung ML, Strebel K, Jeang KT. Human immunodeficiency virus type 1 replication and regulation of APOBEC3G by peptidyl prolyl isomerase Pin1. *J Virol* 2008; **82**: 9928–9936.
60 Satou Y, Nosaka K, Koya Y, Yasunaga JI, Toyokuni S, Matsuoka M. Proteasome inhibitor, bortezomib, potently inhibits the growth of adult T-cell leukemia cells both in vivo and in vitro. *Leukemia* 2004; **18**: 1357–1363.
61 Fan J, Kodama E, Koh Y, Nakao M, Matsuoka M. Halogenated thymidine analogues restore the expression of silenced genes without demethylation. *Cancer Res* 2005; **65**: 6927–6933.

Supplementary Information accompanies the paper on the Oncogene website (http://www.nature.com/onc)

blood 2012 119: 434-444
doi:10.1182/blood-2011-05-357459 originally published online November 28, 2011

HTLV-1 bZIP factor impairs cell-mediated immunity by suppressing production of Th1 cytokines

Kenji Sugata, Yorifumi Satou, Jun-ichirou Yasunaga, Hideki Hara, Kouichi Ohshima, Atae Utsunomiya, Masao Mitsuyama and Masao Matsuoka

Blood (print ISSN 0006-4971, online ISSN 1528-0020), is published weekly by the American Society of Hematology, 2021 L St, NW, Suite 900, Washington DC 20036.

HTLV-1 bZIP factor impairs cell-mediated immunity by suppressing production of Th1 cytokines

Kenji Sugata,[1] Yorifumi Satou,[1] Jun-ichirou Yasunaga,[1] Hideki Hara,[2] Kouichi Ohshima,[3] Atae Utsunomiya,[4] Masao Mitsuyama,[2] and Masao Matsuoka[1]

[1]Laboratory of Virus Control, Institute for Virus Research, Kyoto University, Kyoto, Japan; [2]Department of Microbiology, Kyoto University Graduate School of Medicine, Kyoto, Japan; [3]Department of Pathology, School of Medicine, Kurume University, 67 Asahimachi, Kurume, Fukuoka, Japan; [4]Department of Hematology, Imamura Bun-in Hospital, Kagoshima, Japan

Adult T-cell leukemia (ATL) patients and human T-cell leukemia virus-1 (HTLV-1) infected individuals succumb to opportunistic infections. Cell mediated immunity is impaired, yet the mechanism of this impairment has remained elusive. The *HTLV-1 basic leucine zipper factor* (*HBZ*) gene is encoded in the minus strand of the viral DNA and is constitutively expressed in infected cells and ATL cells. To test the hypothesis that HBZ contributes to HTLV-1–associated immunodeficiency, we challenged transgenic mice that express the *HBZ* gene in CD4 T cells (HBZ-Tg mice) with herpes simplex virus type 2 or *Listeria monocytogenes*, and evaluated cellular immunity to these pathogens. HBZ-Tg mice were more vulnerable to both infections than non-Tg mice. The acquired immune response phase was specifically suppressed, indicating that cellular immunity was impaired in HBZ-Tg mice. In particular, production of IFN-γ by CD4 T cells was suppressed in HBZ-Tg mice. HBZ suppressed transcription from the *IFN-γ* gene promoter in a CD4 T cell–intrinsic manner by inhibiting nuclear factor of activated T cells and the activator protein 1 signaling pathway. This study shows that HBZ inhibits CD4 T-cell responses by directly interfering with the host cell-signaling pathway, resulting in impaired cell-mediated immunity in vivo. (*Blood*. 2012;119(2):434-444)

Introduction

Human T-cell leukemia virus type 1 (HTLV-1) is a retrovirus that mainly infects CD4 T cells,[1] a critical cell population for the host defense against foreign pathogens. HTLV-1 is known as the causal agent of adult T-cell leukemia (ATL),[2-4] a leukemia derived from CD4 T cells, and chronic inflammatory diseases, including HTLV-1-associated myelopathy/tropical spastic paraparesis,[5,6] alveolitis,[7] and uveitis. It has also been recognized that HTLV-1 infection is complicated by opportunistic infections caused by *Pneumocystis jiroveci*, herpes zoster virus, cytomegalovirus, or *Strongyloides stercoralis*.[8] However, the mechanism by which HTLV-1 causes immune deficiency has remained unknown.

Another human pathogenic retrovirus, HIV, replicates vigorously in vivo and produces a large number of virions. As a result of abundant viral production, HIV-infected CD4 T cells proceed to apoptosis, a phenomenon that eventually results in AIDS. In contrast, HTLV-1 increases its copy number primarily in the form of a provirus, by promoting the clonal proliferation of infected host CD4 T cells.[9,10] Despite this opposite effect on CD4 T-cell homeostasis compared with HIV, HTLV-1 infection and ATL are frequently accompanied by a deficiency of cellular immunity resembling that seen with AIDS.

HTLV-1 encodes several regulatory and accessory genes in the viral genome.[1,11] The viral proteins expressed by the integrated provirus control viral gene transcription and induce host cell proliferation, enabling HTLV-1 to achieve persistent infection. Among the viral genes of HTLV-1, *HTLV-1 bZIP factor* (*HBZ*), which is encoded in the minus strand,[12] is a constitutively expressed viral gene.[13] It has been reported that there are 2 major transcripts of the *HBZ* gene: spliced HBZ (sHBZ) and unspliced HBZ (usHBZ).[14] Based on the findings that sHBZ is more abundantly expressed than usHBZ[15] and that sHBZ has a functionally stronger effect than usHBZ,[16] we focused on sHBZ in this study.

Recently, we have reported that sHBZ expression increases the number of regulatory T cells (Tregs) by inducing transcription of the *Foxp3* gene in transgenic mice that express the *HBZ* gene in CD4 T cells (HBZ-Tg mice).[17] An increase in Tregs might be implicated in the immunodeficiency observed in ATL patients. Furthermore, previous studies have reported that HBZ suppresses host cell-signaling pathways that are critical for T-cell receptor signaling in the immune response, such as the NF-κB[18] and AP-1 pathways.[19] These findings led us to hypothesize that HBZ might have important roles in the dysregulation of cellular immunity associated with HTLV-1 infection.

To verify this hypothesis, we used HBZ-Tg mice that express sHBZ in CD4 T cells and studied well-established infection models of 2 pathogens. The first model involves intravaginal viral infection with herpes simplex virus type-2 (HSV-2). IFN-γ production by CD4 T cells is critical for the exclusion of HSV-2 from the host.[20,21] The other model involves infection with the Gram-positive intracellular bacterium, *Listeria monocytogenes* (LM), which is known as an opportunistic pathogen. In LM infection, CD4 T cells play pivotal roles in the acquired immune response by producing IFN-γ and inducing the activation of macrophages, which eliminate LM

Submitted May 27, 2011; accepted November 13, 2011. Prepublished online as Blood First Edition paper, November 28, 2011; DOI 10.1182/blood-2011-05-357459.

The online version of this article contains a data supplement.

The publication costs of this article were defrayed in part by page charge payment. Therefore, and solely to indicate this fact, this article is hereby marked "advertisement" in accordance with 18 USC section 1734.

by phagocytosis and subsequent bactericidal activity.[22,23] Indeed, previous reports have shown that some ATL patients are infected with these 2 pathogens.[24,25] Using these 2 infection models, we demonstrated that sHBZ suppresses cell-mediated immunity. Furthermore, we determined the molecular mechanism of this HBZ-mediated immune suppression.

Methods

Mice

Wild-type C57BL/6J mice were purchased from CREA Japan. Transgenic mice expressing the *sHBZ* gene under control of the CD4 promoter/enhancer/silencer have been described previously.[13] All HBZ-Tg mice were heterozygotes for the transgene. All mice used in this study were maintained in a specific pathogen-free facility and handled according to protocols approved by Kyoto University.

Herpes simplex virus type 2 infection

The HSV-2 wild-type strain UW268 and thymidine kinase (TK)-negative strain UWTK (a gift from T. Suzutani, Fukushima Medical University) used in this study were propagated and titrated on Vero cells.[26] Acyclovir was used for propagation of UWTK to block emergence of TK^+ revertant. To increase their susceptibility to HSV-2, we injected mice subcutaneously with medroxyprogesterone acetate, Depo-provera (Sigma-Aldrich), (2 mg/mouse). Five days after this hormone injection, mice were anesthetized using Avertin (Sigma-Aldrich), preswabbed with a type 2 Calgiswab (Puritan), and inoculated intravaginally with 10^3 or 10^4 plaque-forming units (PFU) of UW268. For studies of secondary infection, mice were first immunized intravaginally with 10^6 PFU of UWTK, and 4 weeks later, they were inoculated intravaginally with 10^5 PFU of UW268. Vaginal secretions were collected by 3 pipettings with 15 μL of PBS, swabbed with a Calgiswab, and added to 955 μL of 5% FCS-DMEM and stored at −80°C. HSV-2 titers were determined by plaque assay on Vero cells. Five days after primary infection, lavage fluid from the vaginal tract was harvested similarly by 3 pipettings with 20 μL of PBS.

At 6 days after infection, the vaginal tissues of infected mice were fixed in 10% formalin in phosphate buffer and embedded in paraffin. H&E staining was performed according to standard procedures. The presence of HSV-2 antigen in tissues was detected using rabbit polyclonal anti–herpes simplex virus type 2 (Dako North America). Images were captured using a Provis AX80 microscope (Olympus) equipped with OLYMPUS DP70 digital camera, and detected using a DP manager system (Olympus; original total magnification ×200).

Splenic CD4 T cells from HSV-2 primary-infected mice were stimulated in a 96-well plate coated with CD3 mAb (1 μg/mL) and CD28 mAb (1 μg/mL) for 24 hours. For antigen specific stimulation, CD4 T cells were cocultured for 48 hours in the presence of irradiated T cell–depleted splenocytes as antigen-presenting cell (APC) and heat-inactivated HSV-2 (heat inactivated at 56°C for 2 hours) at a multiplicity of infection of 1. Supernatant was collected and stored at −20°C until assay.

Evaluation of resistance and immune response to LM in mice

Wild-type LM strain EGD was used in this study. The bacterial suspension was prepared as described previously.[27] For primary infection, mice were inoculated intravenously with 10^3 colony-forming units (CFUs) of LM and the bacterial burden in the spleen was determined on day 2 or 5 after infection.

For studies of secondary infection, mice were immunized intravenously with 10^3 CFUs of LM. From day 3 through day 6.5 after immunization, the drinking water supplemented with ampicillin (2 mg/mL) was given to clear any remaining LM. On day 7, mice were challenged with 10^6 CFUs of LM, and the spleens and sera were harvested after 3 or 12 hours. Spleens were homogenized in PBS, and the number of viable bacteria was determined by plating 10-fold serial dilutions on tryptic soy agar plates and counting the CFUs.

For cytometric assays, immunized mice were re-inoculated with 10^7 CFUs of LM. Splenocytes were harvested after 12 hours, cultured in the presence of protein transport inhibitor for 6 hours, and evaluated by the FACSCanto II (BD Biosciences) for cell surface and intracellular markers.

To determine the functional development of CD4 T cells in immunized mice, we purified splenic CD4 T cells and then stimulated them in a 96-well plate coated with CD3 mAb and CD28 mAb. For LM specific stimulation, CD4 T cells were cocultured with mouse bone marrow–derived macrophages (BMDMs) differentiated in the presence of 100 ng/mL of M-CSF and pulsed with viable LM at a multiplicity of infection of 10. Supernatant after stimulation for 24 hours was collected and stored at −20°C until assay.

Analysis of virus vector-transduced CD4 T cells

Retroviral transduction was performed as described previously.[17] The spliced HBZ gene was cloned into a retroviral vector, pMXs-Ig (a gift from T. Kitamura, The University of Tokyo), to generate pMXs-Ig-HBZ. This plasmid DNA was transfected into the packaging cell line, Plat-E. For retroviral transduction, $CD25^-CD4^+$ cells were enriched by a CD4 enrichment kit (BD Biosciences PharMingen) and were activated by anti-CD3 Ab (0.5 μg/mL) and rIL-2 (50 U/mL) in the presence of T cell–depleted and x-irradiated (20 Gy) C57BL/6J splenocytes as APCs in 12-well plates. After 16 hours, activated T cells were transduced with viral supernatant in the presence of 4 μg/mL polybrene and centrifuged at 1700*g* for 60 minutes. Then, transduced CD4 T cells were stimulated by phorbol 12-myristate 13-acetate (PMA; 50 ng/mL) and ionomycin (1 μg/mL) or plate-coated CD3 mAb (1 μg/mL) and CD28 mAb (1 μg/mL) in the presence of protein transport inhibitor and analyzed by a flow cytometry as shown in Figure 3. Dead cells were excluded using forward and side scatter and LIVE/DEAD Fixable Dead Cell Stain Kit (Invitrogen) by flow cytometry. Thereafter, intracellular cytokines were measured.

For generation of the lentivirus vector, sHBZ cDNA was cloned into pCS2-EF-GFP (a gift from H. Miyoshi, RIKEN BioResource Center) as previously described.[13] In brief, 293FT cells were cotransfected with the lentivirus vector, pCMV-Δ8/9 and pVSVG and supernatant containing virus was used for transduction. The lentivirus titer was determined on 293FT cells.

Empty vectors that express only GFP were used as controls for retroviral and lentiviral transductions.

IFN-γ promoter assay

Nucleotides −670 to +64 of the IFN-γ promoter region were amplified by PCR using human genomic DNA as a template, and cloned into pGL4.22 (Promega). The PathDetect pAP-1-Luc and pNFAT-Luc Cis-Reporter Plasmids were purchased from Promega. Transfection and luciferase assay were performed according to supplemental Methods (available on the *Blood* Web site; see the Supplemental Materials link at the top of the online article).

ChIP assay

sHBZ-expressing Jurkat cells were stimulated with PMA and ionomycin. ChIP assay was performed as reported previously.[28] ChIP DNA samples were subjected to the StepOnePlus real-time PCR system using Power SYBR Green PCR Master Mix (Applied Biosystems). The sequences of the primers for the human IFN-γ promoter were: 5′-TACCAGGGC-GAAGTGGGGAG-3′ (sense) and 5′-GGTTTTGTGGCATTTGGGTG-3′ (anti-sense).

Statistical analysis

For in vitro and in vivo experiments, multiple data comparisons were performed using the Student unpaired *t* test.

Results

High susceptibility of HBZ-Tg mice to HSV-2 infection

We first evaluated the susceptibility of HBZ-Tg mice to HSV-2 infection. Recently, we reported that HBZ-Tg mice frequently develop T-cell lymphoma and dermatitis after 10 weeks.[17] Therefore, HBZ-Tg mice without skin symptoms at 7 to 10 weeks of age were used in this study. It has been reported that the host immune response against primary HSV-2 infection can be divided into 2 stages: the innate immune response plays a dominant role by day 2 after infection, whereas cellular immunity plays an important role later, after day 5 after infection.[29] IFN-γ production by CD4 T cells is known as a critical factor in the cellular immune response against pathogens.[29] To determine whether cellular immunity is impaired in HBZ-Tg mice, we pretreated HBZ-Tg and non-Tg mice with Depo-provera for efficient infection and inoculated them with HSV-2 through the vaginal route.[30] The viral titer of HSV-2 in the lesion was measured. In this primary infection assay, there was no significant difference in the viral titers between non-Tg and HBZ-Tg mice at day 2 after inoculation (Figure 1A), when innate immunity is responsible for the host defense. In contrast, at day 6 after infection, when acquired immunity becomes important, HBZ-Tg mice showed significantly higher viral titers of HSV-2 than non-Tg mice (Figure 1A). Immunohistochemical analysis revealed that abundant viral antigens were detected in the vaginal epithelial cells and ganglia of HSV-2 challenged HBZ-Tg mice but not in non-Tg mice (Figure 1B).

To explore the mechanism of this immune deficiency, we examined cytokine production by CD4 T cells stimulated with antibodies to CD3 and CD28 or with heat-inactivated HSV-2 and APC. On day 6 after infection, the production of Th1 effector cytokines, including IFN-γ, IL-2, and TNF-α, was significantly reduced in CD4 T cells from HBZ-Tg mice compared with non-Tg mice (Figure 1C). Furthermore, IFN-γ concentration in vaginal wash fluids at day 5 after infection was significantly suppressed in HBZ-Tg compared with non-Tg mice (Figure 1D). When we challenged mice with a 50% lethal dose of HSV-2, the survival rate of non-Tg mice at day 20 after infection was 53%. In contrast, HBZ-Tg mice could not survive a viral challenge at the same dose (Figure 1E).

To study acquired immunity against HSV-2, we immunized and challenged mice as shown in Figure 1F. First, mice were immunized by TK-negative HSV-2 strain, the attenuated mutant of HSV-2, and then they were challenged with wild-type HSV-2. The vaginal virus titer in HBZ-Tg mice at day 3 after challenge was similar to that in nonimmune non-Tg mice (Figure 1F), whereas HSV-2 was not detected in immune non-Tg mice. The difference in viral titer between non-Tg and HBZ-Tg mice was much more remarkable in these secondary infection experiments than in the previous primary infection experiments, implicating impaired acquired immunity in HBZ-Tg mice. These results demonstrate that expression of sHBZ in CD4 T cells induces a deficiency in the immune response against HSV-2 and impairs the production of IFN-γ, IL-2, and TNF-α.

HBZ-Tg mice have an impaired T cell–dependent immune response to LM

We next evaluated the susceptibility of HBZ-Tg mice to infection with LM via an intravenous route. As with HSV-2 infection, production of IFN-γ by CD4 T cells plays a crucial role in the growth inhibition and elimination of LM in vivo.[31,32] On day 2 or 5 after primary infection with LM, we removed spleens and evaluated the bacterial burdens in the organs. The number of LM recovered from HBZ-Tg spleen on day 2 was comparable to that from non-Tg mice, yet the bacterial burden in HBZ-Tg mice at day 5 was higher than that in non-Tg mice (Figure 2A), suggesting a reduced protection in HBZ-Tg mice against LM, especially when acquired immunity is being established. We next a performed secondary infection experiment to evaluate the T cell–dependent immunity that developed after primary infection. Non-Tg mice immunized with a small dose of LM and later challenged with a high dose exhibited a significant level of bacterial elimination 12 hours after challenge compared with nonimmunized mice (Figure 2B). By contrast, such a significant level of bacterial elimination was not observed in immunized HBZ-Tg mice (Figure 2B), indicating that acquired LM-specific immunity is impaired in HBZ-Tg mice.

Characterization of cytokine production in the LM-infected mice

We next measured the concentration of several cytokines in the sera and homogenized spleen supernatant of HBZ-Tg and non-Tg mice during secondary infection with LM. IFN-γ, TNF-α, IL-2, IL-6, and IL-10 were decreased in HBZ-Tg mice (Figure 2C) compared with non-Tg mice. On the other hand, IL-12, which is mainly secreted by APCs, was increased in HBZ-Tg at 12 hours. To explore whether impaired production of Th1 cytokines by CD4 T cells is responsible for the decrease in levels of IFN-γ, TNF-α, and IL-2 in the serum, we enriched CD4 T cells from the spleens of immunized mice and then stimulated the cells ex vivo nonspecifically (with mAbs to CD3 and CD28) or specifically (with BMDMs pulsed with viable LM). The ability of CD4 T cells from HBZ-Tg mice to produce IFN-γ and IL-2 in response to either kind of stimulation was markedly impaired compared with that of cells from non-Tg mice (Figure 2D). In contrast, a considerable amount of TNF-α production was detected in tests of both HBZ-Tg and non-Tg CD4 T cells after stimulation with LM-pulsed BMDMs. However, this level of TNF-α was almost comparable with that observed in the culture of LM-pulsed BMDMs alone (Figure 2D). Therefore, the TNF-α detected in this experiment was probably produced by the macrophages, not by the CD4 T cells. These results strongly suggest that the ability of CD4 T cells to produce Th1 cytokines is impaired in HBZ-Tg mice.

Because IFN-γ is reported to play a pivotal role in the acquired protection of mice against LM,[22,23] we focused on IFN-γ production by LM-specific CD4 T cells. Splenic cell suspensions were prepared from 2 groups of mice immunized and challenged according to the protocol shown in Figure 2B. Cells were cultured for 6 hours in the presence of protein transport inhibitor and then subjected to flow cytometric analysis for IFN-γ production by intracellular cytokine staining. The number of IFN-γ–producing CD4 T cells in HBZ-Tg mice was remarkably reduced compared with that in non-Tg mice (Figure 3A). In contrast, IFN-γ production by CD8 T cells showed no significant difference between non-Tg and HBZ-Tg mice (Figure 3A). In addition, there were no differences between HBZ-Tg mice and control littermates in both total and $CD4^+$ splenocytes (supplemental Figure 1).

We recently reported that the proportion of $Foxp3^+$ $CD4^+$ T cells is increased in HBZ-Tg mice.[17] A previous study reported that Foxp3 expression inhibits the production of IFN-γ,[33] suggesting that a decreased proportion of effector T cells in HBZ-Tg mice might be responsible for the low number of IFN-γ–producing CD4

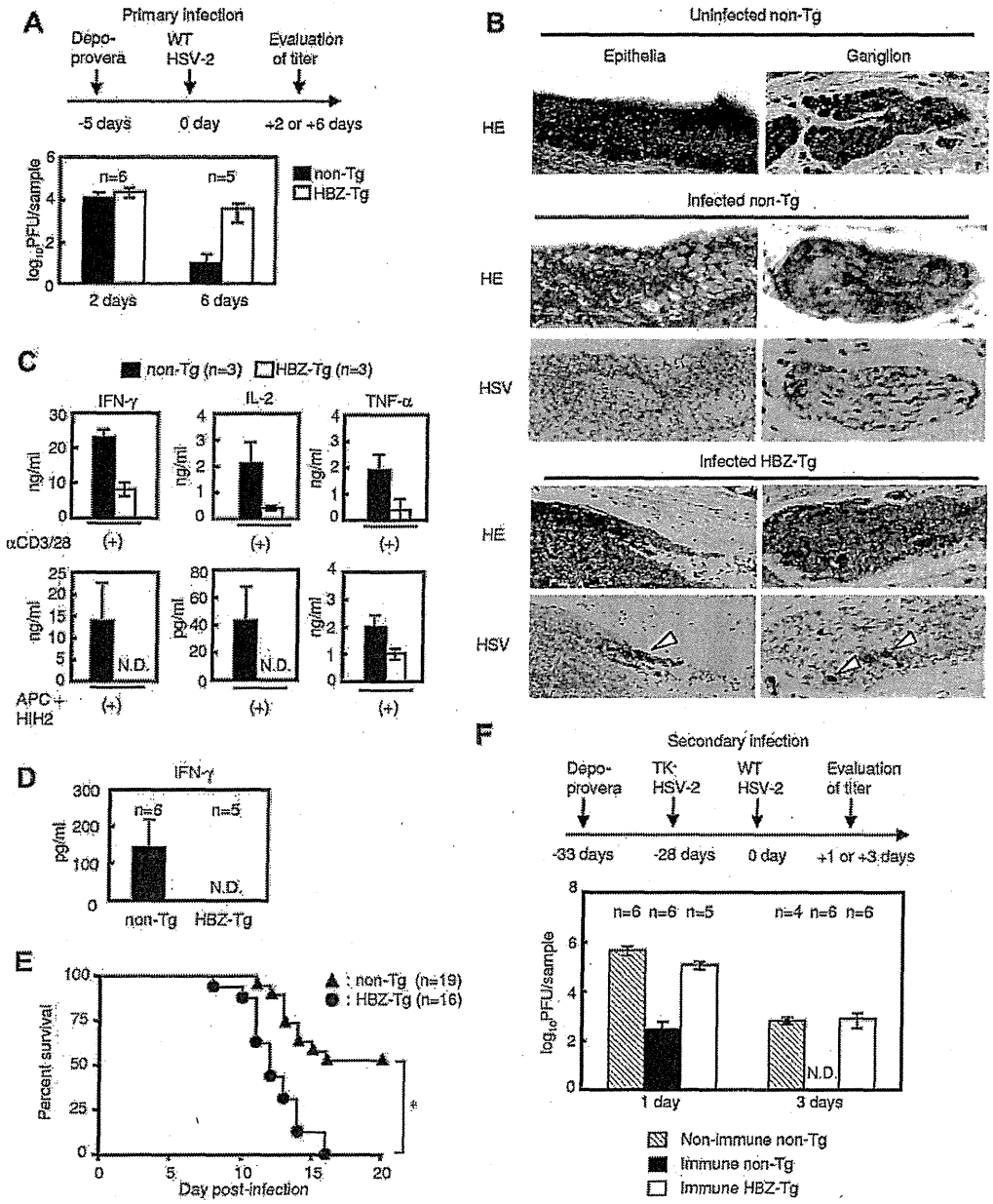

Figure 1. Transgenic mice expressing sHBZ in CD4 T cells are highly susceptible to intravaginal infection with HSV-2. (A) Virus titer in vaginal washes in primary infection. (B) Histologic analysis of epithelia and ganglion in vaginal tissue from mice infected with HSV-2. Uninfected vaginal tissues are presented as controls. HE indicates H&E stain; and HSV, immunohistochemical analysis for the viral antigen. Arrowheads indicate HSV-2–positive cells. (C) Cytokine production by splenic CD4 T cells from mice infected with 10^4 plaque-forming units (PFU) of HSV-2. Cells were stimulated with mAbs to CD3 and CD28 or APC plus heat-inactivated HSV-2 (HIH2) in ex vivo culture. (D) IFN-γ concentration in vaginal wash fluid harvested at day 5 after infection. (E) Survival curve of non-Tg or HBZ-Tg mice infected with 10^5 PFU of HSV-2. *$P < .05$ (log-rank test). (F) Viral titer in vaginal washes during HSV-2 secondary infection. To evaluate adaptive immunity against HSV-2 infection, mice were immunized and infected with the virus as shown in the upper panel. Bars represent the mean ± SD of all mice per genotype. Two or 3 independent experiments have been performed. N.D. indicates not detected.

T cells. However, the impairment of IFN-γ production was still observed in the Foxp3-negative effector CD4 T-cell population (Figure 3B), indicating that the reduction in IFN-γ production is independent of Foxp3 expression. These results collectively indicate that transgenic expression of sHBZ in CD4 T cells results in a reduction in effector cytokine production by CD4 T cells.

sHBZ directly inhibits IFN-γ production in a CD4 T cell–intrinsic manner

To determine whether sHBZ-mediated IFN-γ suppression was induced by a cell-intrinsic effect of sHBZ in CD4 T cells or by a dysregulated immunologic status in vivo indirectly caused by sHBZ expression, we used a retrovirus vector to express sHBZ in naive CD4 T cells. Wild-type CD4 T cells transduced with sHBZ showed lower IFN-γ production than empty vector-transduced cells (Figure 4A-B), demonstrating that sHBZ directly suppresses IFN-γ production in CD4 T cells. It is noteworthy that sHBZ suppressed IFN-γ production in human CD4 T cells as well as mouse T cells. This suppression was not limited to IFN-γ but was also observed for TNF-α (Figure 4C) and IL-2 (Figure 4D). Expression level of the *HBZ* gene transcript was much higher than that of HBZ-Tg mice (supplemental Figure 2). IL-4 production was